

CPT-97/P.3638  
UAB-FT-443

# Matching Long and Short Distances in Large- $N_c$ QCD

Santiago Peris<sup>a</sup>, Michel Perrottet<sup>b</sup> and Eduardo de Rafael<sup>b</sup>

<sup>a</sup> Grup de Física Teòrica and IFAE  
Universitat Autònoma de Barcelona, 08193 Barcelona, Spain.

and

<sup>b</sup> Centre de Physique Théorique  
CNRS-Luminy, Case 907  
F-13288 Marseille Cedex 9, France

*Submitted to JHEP*

## Abstract

It is shown, with the example of the experimentally known Adler function, that there is no matching in the intermediate region between the two asymptotic regimes described by perturbative QCD (for the very short-distances) and by chiral perturbation theory (for the very long-distances). We then propose to consider an approximation of large- $N_c$  QCD which consists in restricting the hadronic spectrum in the channels with  $J^P$  quantum numbers  $0^-$ ,  $1^-$ ,  $0^+$  and  $1^+$  to the lightest state and to treat the rest of the narrow states as a perturbative QCD continuum; the onset of this continuum being fixed by consistency constraints from the operator product expansion. We show how to construct the low-energy effective Lagrangian which describes this approximation. The number of free parameters in the resulting effective Lagrangian can be reduced, in the chiral limit where the light quark masses are set to zero, to just one mass scale and one dimensionless constant to all orders in chiral perturbation theory. A comparison of the corresponding predictions, to  $\mathcal{O}(p^4)$  in the chiral expansion, with the phenomenologically known couplings is also made.

# 1 Introduction

We shall be concerned with Green's functions of colour singlet operators which are bilinear in the light quark fields. There are at present two asymptotic regimes where QCD is a predictive theory for these Green's functions: the short-distance regime where the external momenta are deep euclidean in regions of non-exceptional momenta [1], and the very long-distance regime where the external momenta are very soft. The behaviour of the Green's functions in the short-distance regime can be successfully predicted via perturbation theory in powers of the QCD running coupling constant (pQCD). In the chiral limit where the light quark masses are set to zero, the behaviour in the short-distance regime is then governed by only one mass scale, e.g. the  $\Lambda_{\overline{\text{MS}}}$  parameter for three flavours.

The way that QCD predicts the behaviour of the Green's functions in the long-distance regime is not so straightforward. At very low energies, the sole input of the property of spontaneous breakdown of the chiral  $SU_L(3) \times SU(3)_R$  invariance of the QCD Lagrangian with massless  $u, d, s$  quarks, allows one to set up a well defined theoretical framework [2–6] known as Chiral Perturbation Theory ( $\chi$ PT). This is formulated in terms of an effective Lagrangian that describes, at low energies, the strong interactions of the Goldstone modes associated with spontaneous chiral symmetry breaking. The behaviour of the Green's functions in the very long-distance regime is then predicted by this effective Lagrangian as an expansion in powers of momenta. This, however, comes at the expense of introducing an increasing number of local operators of higher dimension with unknown couplings which build the effective Lagrangian at higher orders in the chiral expansion. [Some of these local operators act as counterterms in the loop expansion generated by the lower order terms.] At  $\mathcal{O}(p^6)$  in the chiral expansion the number of independent local operators is already of the order of a hundred [7]. Although in principle their couplings are fixed from QCD, their calculation demands a genuine knowledge of non-perturbative QCD properties. In certain circumstances one can relate these low-energy constants to a sufficient amount of independent experimental observables which determine them and many successful predictions have been made this way<sup>1</sup>. [This is the orthodox methodology of the  $\chi$ PT science.] However, as higher orders in the chiral expansion are required, it often happens that there is simply no model independent way to fix all the couplings. In practice the onset of this situation is at  $\mathcal{O}(p^6)$  in the chiral Lagrangian for the strong interactions and already at  $\mathcal{O}(p^4)$  in the sector of the non-leptonic weak interactions. If one wishes to make progress here, one clearly needs to find a good theoretical approximation as a substitute for full fledged QCD.

An interesting question one may ask is: what is the *matching* of the two asymptotic regimes which we have just described? This is precisely the question which we wish to discuss in this paper. For simplicity we shall illustrate most of this discussion with a specific Green's function, the so called Adler function (see section 2 below for definitions), but many of the features presented here are rather generic. We claim that the direct matching is in fact extremely poor; even when non-perturbative short-distance power corrections à la SVZ [11] are retained. Once more we find that if one wishes to make progress in the quality of the matching between the pQCD short-distance behaviour and the  $\chi$ PT behaviour which is only operational at very long-distances, one clearly needs a good theoretical approximation as a substitute for full fledged QCD.

As a first step in this direction we shall consider QCD in the limit of a large number of

---

<sup>1</sup>See e.g. the review articles in refs. [8–10]

colours [13–17]. This limit, which following ’t Hooft’s notation we shall term  $\text{QCD}(\infty)$  for short, offers a convenient starting point where one can hope to discuss fruitfully the aforementioned matters since it is still rich enough to share with QCD its most relevant non-perturbative features. Among them, a very important one, is the fact that  $\text{QCD}(\infty)$  has the correct pattern of spontaneous chiral symmetry breaking [18, 19], provided that the property of confinement still persists in going from QCD to  $\text{QCD}(\infty)$ . The advantage of the large- $N_c$  limit is the emergence of narrow meson states in the Green’s functions. The disadvantage is that the number of narrow states is infinite and they appear at all energy scales, even when the euclidean momenta are large enough that a perturbative treatment should be adequate. Obviously, a perturbative description, when possible, is more predictive than an infinite tower of narrow states with masses and decay constants which are a priori unknown.

We propose to consider an approximation to  $\text{QCD}(\infty)$  which consists in restricting the hadronic spectrum in the channels with  $J^P$  quantum numbers  $0^-$ ,  $1^-$ ,  $0^+$  and  $1^+$  to the lowest energy state and in treating the rest of the narrow states as a  $\text{QCD}(\infty)$  perturbative continuum; the onset of the continuum being fixed by consistency constraints from the operator product expansion (OPE) as we shall discuss. The reason why we limit ourselves to this simple hadronic spectrum is that, in the large- $N_c$  limit, this is the minimal structure compatible with spontaneous chiral symmetry breaking [19]. The traditional successes of “vector meson dominance” in describing low energy hadron phenomenology guarantees that this approximation, which we shall call “lowest meson dominance (LMD) approximation to large- $N_c$  QCD”, should be rather reasonable <sup>2</sup>. The immediate question which then arises is the following: is there an effective Lagrangian formulation which explicitly exhibits the properties of  $\text{QCD}(\infty)$  in the LMD approximation? We shall show that there is indeed such an effective Lagrangian. The effective Lagrangian in question can be obtained starting from a modified version of an extended Nambu–Jona-Lasinio type Lagrangian (ENJL) which has been very much discussed in the literature <sup>3</sup>. The modifications, however, are highly non trivial because they require the presence of an infinity of local operators which, however, have known couplings. The couplings of the new operators are known because they are fixed by the requirement that they remove, order by order in the chiral expansion, the effects of *non-confining*  $Q\bar{Q}$  discontinuities produced by the initial ENJL *ansatz*. The resulting Lagrangian when the quark fields are integrated out is a non-linear sigma type Lagrangian with degrees of freedom corresponding to the Goldstone fields and also to Vector, Axial–Vector, and Scalar fields. The *matching* of the two-point functions of this effective Lagrangian to their QCD short-distance behaviour can be systematically implemented. However, for Green’s functions beyond two-point functions, the removal of the *non-confining*  $Q\bar{Q}$  discontinuities produced by the initial ENJL *ansatz* is not enough to guarantee in general the correct *matching* to the leading QCD short-distance behaviour and further local operators have to be included. In the sector of Vector and Axial–Vector couplings, and after the *matching* with the QCD short-distance behaviour from the OPE for three-point functions is implemented [26], the resulting low-energy Lagrangian to  $\mathcal{O}(p^4)$  in the chiral expansion coincides with the class of Lagrangians discussed in ref. [27]. The advantage, however, with respect to a purely phenomenological description in terms of chiral effective Lagrangians which include resonances

---

<sup>2</sup>If necessary, one could also add further states, (see e.g. ref. [20] for a recent discussion of a possible description of the  $\pi(1300)$ .) However, as we shall see, the phenomenological success of the LMD approximation indicates that, to a good approximation, these higher states play a minor rôle in the dynamics of the low-energy effective Lagrangian.

<sup>3</sup>See e.g. refs. [21–25] and references therein

as discussed e.g. in refs. [28–31] and references therein, is that in the LMD approximation to  $\text{QCD}(\infty)$ , the number of free parameters can be reduced to just one mass scale and one dimensionless parameter to all orders in  $\chi\text{PT}$ .

## 2 The Adler Function

We are concerned with two-point functions

$$\Pi_{\mu\nu}(q)_{ab} = i \int d^4x e^{iq \cdot x} < 0|T\{V_\mu^a(x)V_\nu^b(0)\}|0> \quad (2.1)$$

of vector quark currents

$$V_\mu^a(x) = \bar{q}(x)\gamma_\mu \frac{\lambda^a}{\sqrt{2}} q(x), \quad (2.2)$$

where  $\lambda^a$  are Gell-Mann matrices ( $\text{tr} \lambda^a \lambda^b = 2\delta_{ab}$ ) acting on the flavour triplet of  $u, d, s$  light quarks. In the chiral limit where the light quark masses are set to zero, these two-point functions depend only on one invariant function ( $Q^2 = -q^2 \geq 0$  for  $q^2$  spacelike)

$$\Pi_{\mu\nu}(q)_{ab} = (q_\mu q_\nu - g_{\mu\nu} q^2) \Pi(Q^2) \delta_{ab}. \quad (2.3)$$

In QCD, the invariant function  $\Pi(Q^2)$  obeys a once-subtracted dispersion relation and it is conventional to choose the subtraction at  $Q^2 = 0$ :

$$\Pi(Q^2) = \Pi(0) - Q^2 \int_0^\infty \frac{dt}{t} \frac{1}{t+Q^2} \frac{1}{\pi} \text{Im}\Pi(t). \quad (2.4)$$

The Adler function [33] is defined as the derivative of the invariant function  $\Pi(Q^2)$  i.e.,

$$\mathcal{A}(Q^2) = -Q^2 \frac{d\Pi(Q^2)}{dQ^2}, \quad (2.5)$$

and therefore, its relation to the spectral function  $\frac{1}{\pi} \text{Im}\Pi(t)$  does not depend on the choice of the subtraction

$$\mathcal{A}(Q^2) = \int_0^\infty dt \frac{Q^2}{(t+Q^2)^2} \frac{1}{\pi} \text{Im}\Pi(t). \quad (2.6)$$

### 2.1 Short-Distance Behaviour

The Adler function obeys a homogeneous renormalization group equation, and it has been computed in pQCD (in the  $\overline{MS}$  renormalization scheme) up to  $\mathcal{O}(\alpha_s^3)$ , with the result [34, 35]

$$\begin{aligned} \mathcal{A}(Q^2)|_{\text{pQCD}} = & \frac{N_c}{16\pi^2} \frac{4}{3} \left\{ 1 + \frac{\alpha_s(\mu^2)}{\pi} + \left[ F_2 + \frac{\beta_1}{2} \log \frac{Q^2}{\mu^2} \right] \left( \frac{\alpha_s(\mu^2)}{\pi} \right)^2 \right. \\ & \left. + \left[ F_3 + (F_2\beta_1 + \frac{\beta_2}{2}) \log \frac{Q^2}{\mu^2} + \frac{\beta_1^2}{4} \left( \frac{\pi^2}{3} + \log^2 \frac{Q^2}{\mu^2} \right) \right] \left( \frac{\alpha_s(\mu^2)}{\pi} \right)^3 + \mathcal{O}(\alpha_s^4) \right\}, \end{aligned} \quad (2.7)$$

where

$$\beta_1 = \frac{n_f}{3} - \frac{11}{6} N_c, \quad \beta_2 = -\frac{51}{4} + \frac{19}{12} n_f, \quad (2.8)$$

$$F_2 = 1.986 - 0.115 n_f, \quad F_3 = -6.637 - 1.200 n_f - 0.005 n_f^2, \quad (2.9)$$

and  $n_f$  the number of light quark flavors. The behaviour of the Adler function as a function of  $Q^2$  predicted by pQCD is shown in Fig. 1. The plot in Fig. 1 corresponds to the choice  $\mu^2 = Q^2$  in eq. (2.7), with  $\alpha_s(Q^2)$  the solution to the implicit equation

$$\frac{2\pi}{-\beta_1 \alpha_s(Q^2)} = \left( \log \frac{Q^2}{\Lambda^2} \right) \left( 1 - \frac{2\beta_2}{\beta_1^2 \log \frac{\mu^2}{\Lambda^2}} \log \left[ \frac{2\pi}{-\beta_1 \alpha_s(Q^2)} - \frac{2\beta_2}{\beta_1^2} \right] \right), \quad (2.10)$$

which results from solving the running coupling constant renormalization group equation at the two-loop level. Figure 1 clearly shows the asymptotic freedom behaviour:  $\mathcal{A}(Q^2 \rightarrow \infty) = \frac{N_c}{16\pi^2} \frac{4}{3}$ , as well as the fact that at  $Q^2 \lesssim 1 \text{ GeV}^2$  we are already entering a region where non-perturbative effects are likely to be important.

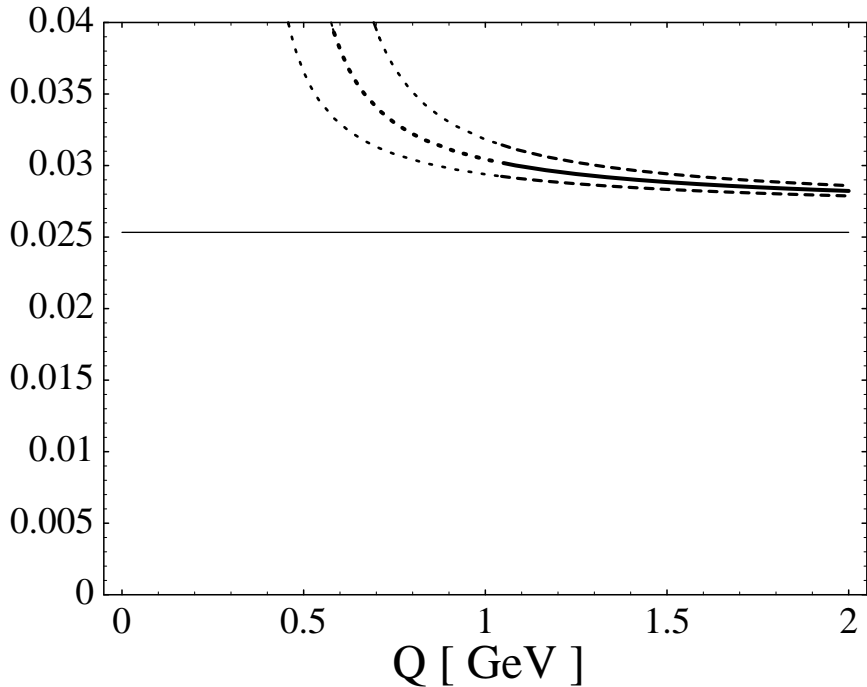


**Fig. 1** The Adler function from perturbative QCD. The dashed lines correspond to  $\Lambda_{\overline{MS}} = (372 \pm 76) \text{ MeV}$  [36, 37].

As first pointed out by Shifman, Vainshtein and Zakharov [11], non-perturbative  $\frac{1}{Q^2}$ -power corrections appear naturally when two-point functions like eq. (2.1) are considered in the physical vacuum within the framework of the operator product expansion (OPE). The leading  $\frac{1}{Q^4}$  and next-to-leading  $\frac{1}{Q^6}$  non-perturbative corrections were calculated in ref. [11]. They depend on the size of the *gluon condensate*, which gives the leading correction to the perturbative result in eq. (2.7):

$$\mathcal{A}(Q^2)_{GG} = \frac{1}{6} \frac{\alpha_s}{\pi} \frac{\langle G_a^{\mu\nu} G_{\mu\nu}^a \rangle}{Q^4}; \quad (2.11)$$

and on the size of *four quark condensates*, which give the next-to-leading power correction to the perturbative result in eq. (2.7):

$$\begin{aligned} \mathcal{A}(Q^2)_{\bar{\psi}\psi\bar{\psi}\psi} &= \left[ -3 \left\langle (\bar{u}\gamma_\mu\gamma_5\lambda^a u - \bar{d}\gamma_\mu\gamma_5\lambda^a d)^2 \right\rangle \right. \\ &\quad \left. - \frac{2}{3} \left\langle (\bar{u}\gamma_\mu\lambda^a u + \bar{d}\gamma_\mu\lambda^a d) \sum_{q=u,d,s} \bar{q}\gamma^\mu\lambda^a q \right\rangle \right] \frac{\pi\alpha_s}{Q^6}. \end{aligned} \quad (2.12)$$

To leading order in the  $1/N_c$ -expansion *four quark condensates* factorize into products of the lowest dimension *quark condensate* with the result

$$\mathcal{A}(Q^2)_{\bar{\psi}\psi\bar{\psi}\psi}^{N_c \rightarrow \infty} = -\frac{28}{3} \frac{\pi\alpha_s}{Q^6} \langle \bar{\psi}\psi \rangle^2. \quad (2.13)$$

The phenomenological determinations of the *gluon condensate* and the *quark condensate* have unfortunately rather big errors. A generous range for the *gluon condensate* which covers most of the determinations is

$$\langle \alpha_s G_a^{\mu\nu} G_{\mu\nu}^a \rangle = (0.08 \pm 0.04) \text{ GeV}^4. \quad (2.14)$$

The *quark condensate* is scale dependent. The values obtained from a variety of sum rules<sup>4</sup>

$$\langle \bar{\psi}\psi \rangle (1 \text{ GeV}^2) = [(-235 \pm 27) \text{ MeV}]^3. \quad (2.15)$$

Using these values, the resulting prediction for the Adler function is shown in Fig. 2.

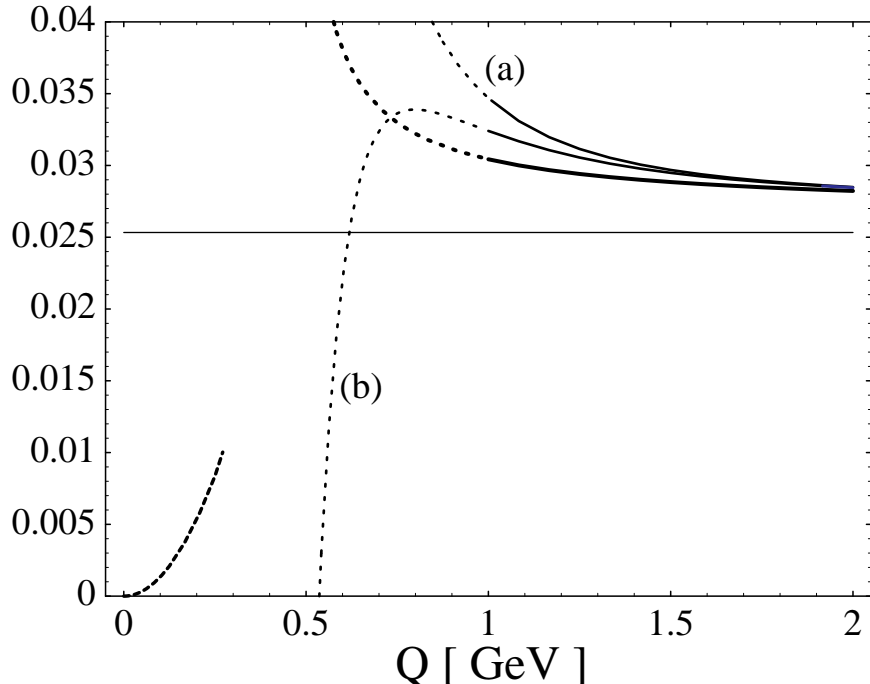


**Fig. 2** The Adler function including (a) the  $\frac{1}{Q^4}$  corrections, (b) the  $\frac{1}{Q^4}$  and  $\frac{1}{Q^6}$  corrections. The dashed line is the VMD prediction corresponding to eq. (2.19) below, valid at low  $Q$ .

<sup>4</sup>See e.g. the recent compilation of sum rule estimates in ref. [12]. Our error in eq. (2.15) is however larger than the one quoted in this reference.

The curve (a) in the figure is the one which results from adding only the  $\frac{1}{Q^4}$ –corrections to the pQCD result shown in Fig. 1; the curve (b) includes both the  $\frac{1}{Q^4}$  and  $\frac{1}{Q^6}$ –corrections. The curves in Fig. 2 clearly show that with the values for the lower dimension *condensates* given in eqs. (2.14) and (2.15), the contribution from the leading and next–to–leading non–perturbative power corrections –at  $Q^2$  values where one can trust the pQCD contributions– turn out to be already quite small. This is due to the empirical fact that the scale of perturbation theory  $\Lambda_{\overline{MS}}$  is rather large (we are using [36, 37]  $\Lambda_{\overline{MS}} = (372 \pm 76)$  MeV in our plots). For values of  $\Lambda_{\overline{MS}}$  as large as that, one is forced to choose  $Q^2 > 1 \text{ GeV}^2$  to trust the perturbative expansion in powers of  $\alpha_s(Q^2)$ , and for  $Q^2 > 1 \text{ GeV}^2$  the power corrections are already quite small.

## 2.2 Long–Distance Behaviour

The behaviour of the invariant function  $\Pi(Q^2)$  in eq. (2.3) at  $Q^2 = 0$  is governed by a combination of two  $\mathcal{O}(p^4)$  coupling constants of the  $\chi$ PT effective Lagrangian:

$$\Pi(Q^2) = -4(2H_1 + L_{10}) + \mathcal{O}(Q^2). \quad (2.16)$$

The constants  $H_1$  and  $L_{10}$  are the coupling constants of the terms

$$\begin{aligned} \mathcal{L}_{\text{eff}}(x) = & \cdots + L_{10} \text{tr} U(x)^\dagger F_R^{\mu\nu}(x) U(x) F_{L\mu\nu}(x) \\ & + H_1 \text{tr} (F_R^{\mu\nu}(x) F_{R\mu\nu}(x) + F_L^{\mu\nu}(x) F_{L\mu\nu}(x)) + \cdots \end{aligned} \quad (2.17)$$

in the effective chiral Lagrangian, where  $F_L$  and  $F_R$  are the field strength tensors associated with external  $v_\mu - a_\mu$  and  $v_\mu + a_\mu$  matrix field sources, and  $U(x)$  the unitary matrix which collects the Goldstone fields ( $U \rightarrow V_R U V_L^\dagger$  under chiral transformations). The Adler function is not sensitive to  $\Pi(0)$ , and hence to  $2H_1 + L_{10}$ . The slope of the Adler function at the origin corresponds therefore to combinations of couplings in  $\chi$ PT which are already of  $\mathcal{O}(p^6)$  and therefore theoretically unknown *a priori*. There are also contributions to the slope of the Adler function from chiral loops involving lower order couplings. These chiral loop contributions are calculable [38], but they are non–leading in the  $1/N_c$ –expansion and therefore we shall ignore them here.

One can make an “educated” guess of the value of the slope of the Adler function at the origin by invoking VMD arguments. In this case it amounts to the assumption that, at low energies, the vector spectral function is dominated by the narrow width pole corresponding to the  $\rho$ –meson

$$\frac{1}{\pi} \text{Im} \Pi(t) \simeq 2f_\rho^2 M_\rho^2 \delta(t - M_\rho^2). \quad (2.18)$$

This leads to the “prediction”

$$\mathcal{A}(Q^2 \rightarrow 0)_{\text{VMD}} = \frac{2f_\rho^2}{M_\rho^2} Q^2 + \mathcal{O}(Q^4), \quad (2.19)$$

and it corresponds to the dashed line starting at  $Q^2 = 0$  which we have plotted in Fig. 2.

We conclude that the only rigorous knowledge we have from QCD about the long–distance behaviour of the Adler function is that it vanishes at  $Q^2 = 0$ , with a slope which is governed by  $\mathcal{O}(p^6)$  terms in  $\chi$ PT and therefore its determination is, at present, model dependent. We

wish to emphasize, however, that the property that it vanishes at  $Q^2 = 0$  is highly non-trivial. There is nothing in the pQCD behaviour in eq. (2.7) which points to that. Although one can find in the literature arguments invoking that  $\alpha_s(Q^2)$  might “freeze” to a constant value when  $Q^2 \rightarrow 0$ , one should be aware that in the case of the Adler function a naïve “freezing argument” contradicts<sup>5</sup> the long-distance QCD behaviour encoded in  $\chi$ PT.

### 2.3 Empirical Determination of the Adler Function

The isovector hadronic spectral function has been determined both from  $e^+e^-$ -annihilation measurements and from hadronic  $\tau$ -decays<sup>6</sup>. We show in Fig. 3 the compilation from the  $\tau$ -data as given in ref. [40], except for the overall normalization.

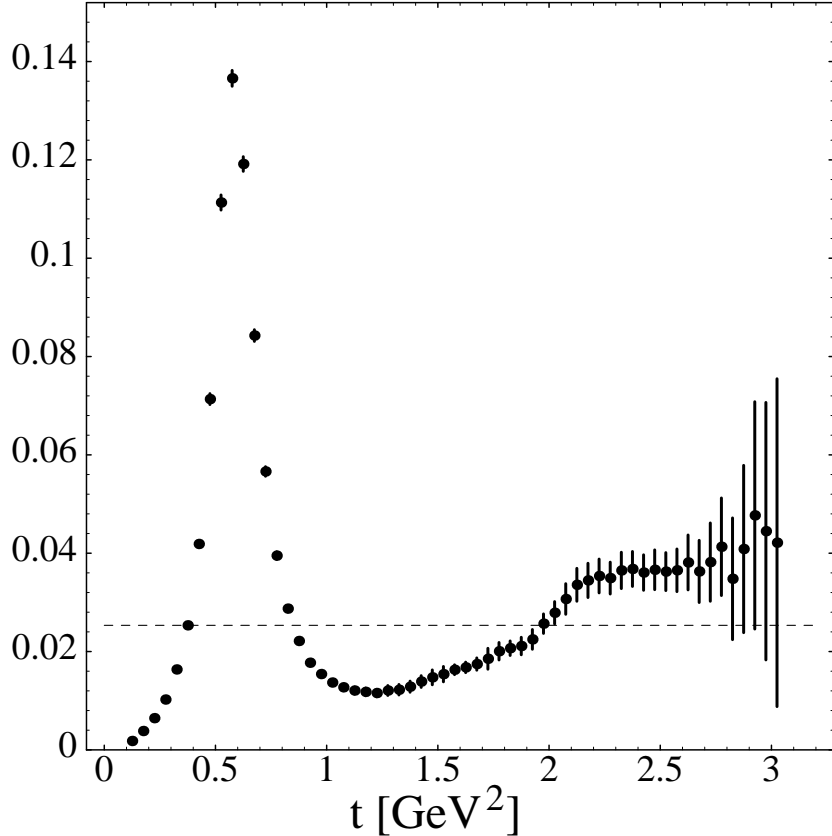


**Fig. 3** The isovector hadronic spectral function from hadronic  $\tau$ -decays. The dashed line is the asymptotic freedom prediction  $\frac{1}{4\pi^2}$ .

The normalization in our Fig. 3 is in accordance with the definition of the spectral function given in eqs. (2.1) to (2.4) above. When extracting the Adler function from experimental data, one is confronted with the question of *matching* to the asymptotic QCD continuum beyond the region accessible to experiment. The concept of *global duality*, as explained in refs. [41, 42], provides the way to do this *matching*. In practice, it consists in introducing an

<sup>5</sup>See the appendix in ref. [39] for further discussion on this point.

<sup>6</sup> For a recent review, where references to the original experiments can be found, see ref. [40].

*ansatz* for the complete spectral function

$$\frac{1}{\pi} \text{Im}\Pi(t) = \frac{1}{\pi} \text{Im}\Pi(t)_{\text{exp.}} \theta(s_0 - t) + \frac{1}{\pi} \text{Im}\Pi(t)_{\text{pQCD}} \theta(t - s_0), \quad (2.20)$$

where  $\frac{1}{\pi} \text{Im}\Pi(t)_{\text{exp.}}$  denotes the hadronic experimental spectral function and  $\frac{1}{\pi} \text{Im}\Pi(t)_{\text{pQCD}}$  the spectral function predicted by pQCD. The onset of the continuum  $s_0$  is then fixed by solving the equation in  $s_0$ :

$$\int_0^{s_0} dt \frac{1}{\pi} \text{Im}\Pi(t)_{\text{exp.}} = \int_0^{s_0} dt \frac{1}{\pi} \text{Im}\Pi(t)_{\text{pQCD}}. \quad (2.21)$$

This equation guarantees that the *matching* between long distances and short distances in the Adler function is consistent with the OPE. Indeed, it can be easily shown that the equation in (2.21) follows from the absence of operators of dimension two<sup>7</sup> in the OPE of the product of current operators which defines the Adler function.

Using the experimental input corresponding to the  $\tau$ -decay data shown in Fig. 3, and the expression<sup>8</sup>

$$\begin{aligned} \int_0^{s_0} dt \frac{1}{\pi} \text{Im}\Pi(t)_{\text{pQCD}} &= \frac{N_c}{16\pi^2} \frac{4}{3} s_0 \left\{ 1 + \frac{\alpha_s(s_0)}{\pi} \right. \\ &+ \left[ F_2 - \frac{\beta_1}{2} \right] \left( \frac{\alpha_s(s_0)}{\pi} \right)^2 + \left[ F_3 - \left( F_2 \beta_1 + \frac{\beta_2}{2} \right) + \frac{\beta_1^2}{2} \right] \left( \frac{\alpha_s(s_0)}{\pi} \right)^3 \left. \right\}, \end{aligned} \quad (2.22)$$

for the pQCD r.h.s. in eq. (2.21) results in the solution

$$s_0 = (1.60 \pm 0.17) \text{ GeV}^2, \quad (2.23)$$

where the error comes from the error on  $\Lambda_{\overline{MS}}$  only. The resulting Adler function is shown in Fig. 4 below.

---

<sup>7</sup> In the presence of quark masses there is in fact a correction term to eq. (2.21) of  $\mathcal{O}(\frac{m^2}{s_0})$  which we are neglecting here.

<sup>8</sup> For the purposes we are interested in here, the evaluation of this integral as a contour integral in the complex  $t$ -plane, as proposed e.g. in ref. [43], does not change significantly the result.

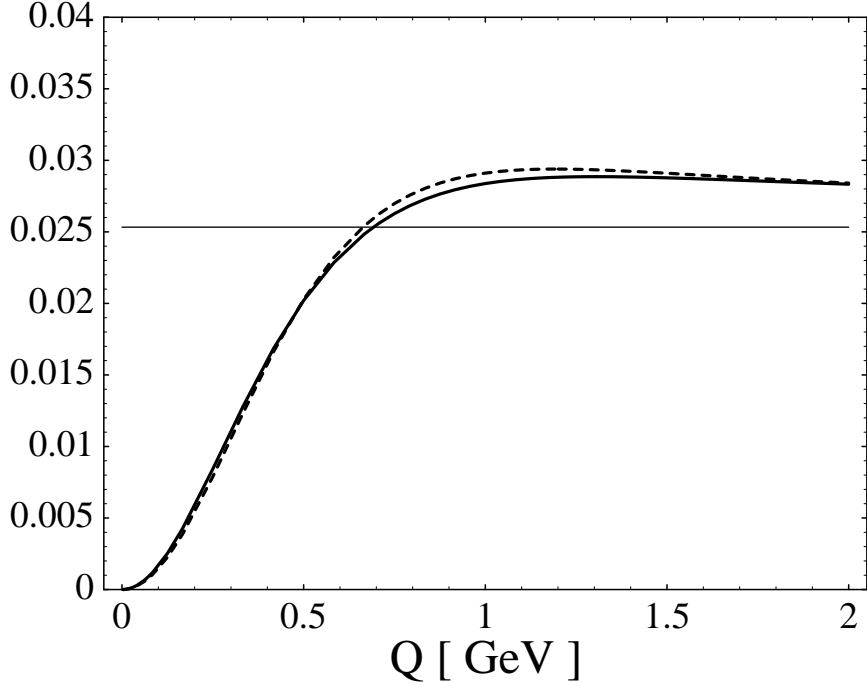


**Fig. 4** The Adler function from experimental data (full line) and from the VMD parameterization (dashed line) in eq.(2.24).

It is interesting to compare the “full experimental” result shown in Fig. 4 with the one obtained from the simplest hadronic parameterization one can think of, which is the one corresponding to a narrow width vector state –the  $\rho(770)$ – plus the corresponding pQCD continuum i.e.,

$$\frac{1}{\pi} \text{Im}\Pi(t) = 2f_\rho^2 M_\rho^2 \delta(t - M_\rho^2) + \frac{1}{\pi} \text{Im}\Pi(t)_{\text{pQCD}} \theta(t - s_\rho). \quad (2.24)$$

The onset of the continuum for this parameterization is at  $s_\rho = (1.53 \pm 0.06) \text{ GeV}^2$ , and the corresponding Adler function is also shown in Fig. 4 -the dashed curve-. Although point by point the two spectral functions in eqs. (2.20) and (2.24) are very different below their continuum onset, the associated Adler functions result in rather similar functions of the euclidean variable  $Q^2$ . It is in this sense that these two spectral functions are *globally dual* [41, 42].

We wish to summarize the basic features which we have learnt in this section.

- The direct matching between  $\chi$ PT and pQCD is very poor, regardless of whether or not one includes non-perturbative power corrections à la SVZ [11]. Including these corrections does not help much because of the empirical fact that  $\Lambda_{\overline{\text{MS}}}$  is large. At the  $Q^2$  values above which we can trust pQCD, the non-perturbative power corrections are already quite small.
- As shown in Fig. 2 there is no matching between the naïve extrapolation of the linear  $Q^2$  behaviour predicted by the first non-trivial order of  $\chi$ PT,  $\mathcal{O}(p^6)$  in this case, and the pQCD prediction with inclusion of the leading  $\frac{1}{Q^4}$  and next-to-leading  $\frac{1}{Q^6}$  non-perturbative power corrections.

- The simplest hadronic parameterization which consists of a narrow-width vector state plus the corresponding pQCD continuum does remarkably well in reproducing the experimental shape of the Adler function. This is very encouraging in view of the LMD approximation to  $\text{QCD}(\infty)$  which we have suggested in the Introduction, namely to consider that the large- $N_c$  spectrum consists of a prominent low-energy narrow state with the rest of the narrow states lumped together as a  $\text{QCD}(\infty)$  perturbative continuum. It is this LMD approximation to  $\text{QCD}(\infty)$  which we are now going to further explore in the following sections.

### 3 Effective Lagrangians and Matching Conditions

Internal quark loops in Green's functions of colour-singlet quark bilinear operators are suppressed in the large- $N_c$  limit. Quark degrees of freedom appear only in the external loop. At low-energies, the external momentum flowing into the quark loop is small. If one “assumes” that the dynamics of the gluons has a characteristic non-perturbative scale  $\Lambda_\chi \gtrsim 1 \text{ GeV}$ <sup>9</sup>, it is natural to think of this quark loop as a low-energy insertion of effective higher-dimensional composite quark operators. These operators will be local at low-energy scales below  $\Lambda_\chi$ . Furthermore, since the physics encoded in these effective operators originates from integrating out degrees of freedom from  $\Lambda_\chi$  to infinity, the QCD  $U(3)_L \times U(3)_R$  flavor symmetry must also be explicitly realized in the effective composite quark operators. Naïvely, one expects  $\Lambda_\chi^2$  and the  $s_0$  of subsec. 2.3 which fixes phenomenologically the onset of the pQCD continuum, to be rather similar.

In perturbation theory one can explicitly see the emergence of these higher dimensional composite operators at very large orders in the QCD coupling constant [39, 44, 45]. Although this is not a proof of the *existence* of these operators, it is nevertheless reassuring to know that there are physical systems which are well described by an analogous mechanism. Indeed, a superconductor is an example of a physical system where the appearance of higher-dimensional fermionic operators in the non-perturbative dynamics is also hinted at by the very large orders of perturbation theory, (see e.g. ref. [46].) It is this kind of reasoning that leads one to consider as a plausible starting *ansatz* to formulate the LMD approximation to  $\text{QCD}(\infty)$ , an effective Lagrangian of the form

$$\begin{aligned} \mathcal{L}_{\text{ENJL}} = & \bar{q}(x) \left[ i\gamma^\mu D_\mu + i(s - i\gamma_5 p) \right] q(x) \\ & + \frac{8\pi^2 G_S}{N_c \Lambda_\chi^2} \sum_{a,b=\text{flavour}} \left( \bar{q}_R^a q_L^b \right) \left( \bar{q}_L^b q_R^a \right) \\ & - \frac{8\pi^2 G_V}{N_c \Lambda_\chi^2} \sum_{a,b=\text{flavour}} \left[ (\bar{q}_L^a \gamma^\mu q_L^b) (\bar{q}_L^b \gamma_\mu q_L^a) + (\text{L} \rightarrow \text{R}) \right] + \dots, \end{aligned} \quad (3.1)$$

where  $D_\mu = \partial_\mu - il_\mu \frac{1-\gamma_5}{2} - ir_\mu \frac{1+\gamma_5}{2}$ ;  $l_\mu = v_\mu - a_\mu$ ,  $r_\mu = v_\mu + a_\mu$ ,  $s$  and  $p$  are external matrix source fields and  $G_S$  and  $G_V$  are dimensionless couplings of  $\mathcal{O}(N_c^0)$ . Summation over colour indices within brackets is understood. This effective Lagrangian is a Nambu–Jona-Lasinio type Lagrangian [21] in its extended version [22–25]. For the sake of brevity we shall refer henceforth to the set of operators explicitly shown in eq. (3.1) as ENJL. The

---

<sup>9</sup> Glueballs, for instance, are expected to have masses  $\gtrsim 1 \text{ GeV}$ .

presence of the two types of four–quark interactions is the minimum required to have non–trivial dynamics in channels with the  $J^P$  quantum numbers  $0^-$ ,  $1^-$ ,  $0^+$ , and  $1^+$ . Taken as it stands this Lagrangian, at leading order in  $1/N_c$  and provided that the coupling  $G_S$  becomes critical ( $G_S > 1$ ), yields the wanted pattern of spontaneous chiral symmetry breaking<sup>10</sup> and reproduces surprisingly well many of the low energy properties of hadron phenomenology [23–25] with only three independent parameters:  $G_S$ ,  $G_V$  and  $\Lambda_\chi$ .

The ENJL Lagrangian, however, has basically two very important drawbacks. On the one hand, although at  $Q^2 = 0$  it produces the correct nonet of Goldstone poles in the S–matrix that are color singlets and have the right flavor quantum numbers; at higher energies it has *unconfined quarks*, whose most evident effect is to create unphysical imaginary parts in Green’s functions. Furthermore, the *unconfined quark–antiquark pairs* produce S–matrix elements which do not obey the mesonic large– $N_c$  counting rules. On the other hand, there is no explanation as yet on how one is supposed to do the *matching* of this effective Lagrangian with short–distance QCD. As we shall see, the two drawbacks are very much related to each other and to the *ellipsis* in eq. (3.1).

### 3.1 The Adler Function of the ENJL–Lagrangian.

The explicit form of the Adler function predicted by the ENJL Lagrangian has been calculated in ref. [24]. It reads

$$\mathcal{A}_{\text{ENJL}}(Q^2) = -Q^2 \frac{d}{dQ^2} \Pi_{\text{ENJL}}(Q^2) = -Q^2 \frac{d}{dQ^2} \left( \frac{\bar{\Pi}(Q^2)}{1 + Q^2 \frac{8\pi^2 G_V}{N_c \Lambda_\chi^2} \bar{\Pi}(Q^2)} \right) , \quad (3.2)$$

where  $\bar{\Pi}(Q^2)$  is given by a loop of constituent free quarks. Since this function is ultraviolet divergent it requires the introduction of a cut–off. We shall later come back to questions of ambiguities from the choice of the cut–off; for the time being, we shall adopt the same proper time regulator as in ref. [24]; then  $\bar{\Pi}(Q^2)$  has the form

$$\bar{\Pi}(Q^2) = \frac{N_c}{16\pi^2} 8 \int_0^1 dx x(1-x) \Gamma(0, x_Q) , \quad (3.3)$$

where  $x_Q \equiv \frac{M_Q^2 + Q^2 x(1-x)}{\Lambda_\chi^2}$  and  $\Gamma(n, \epsilon) \equiv \int_\epsilon^\infty \frac{dz}{z} e^{-z} z^n$  is the incomplete Gamma function. The constituent quark mass  $M_Q$  is the non–trivial solution ( $M_Q \neq 0$ ) to the gap equation

$$\frac{M_Q}{G_S} = M_Q \left[ \exp \left( -\frac{M_Q^2}{\Lambda_\chi^2} \right) - \frac{M_Q^2}{\Lambda_\chi^2} \Gamma(0, \frac{M_Q^2}{\Lambda_\chi^2}) \right] . \quad (3.4)$$

The shape of the Adler function predicted by the ENJL Lagrangian is shown in Fig. 5 (the dotted curve). As the figure clearly shows, ENJL does not interpolate correctly the intermediate region between the very long–distance regime and the short–distance regime; but what is more striking is that it also fails to describe hadronic data already at such low energies as  $Q^2 \lesssim 4M_Q^2$  ( $M_Q \simeq 300$  MeV). The naïve expectation that this effective Lagrangian should

<sup>10</sup> The wanted pattern is the one which produces a sizable quark condensate. Other possible realizations of spontaneous chiral symmetry in QCD have been advocated by J. Stern and collaborators [47–49] and references therein. See however [19].

be appropriate in describing the euclidean behaviour of Green's functions up to  $Q^2 \sim \Lambda_\chi^2$ , (since this is after all the scale that appears in the denominators of the composite operators in eq. (3.1),) has not been fulfilled<sup>11</sup>. This failure can be delayed to slightly higher  $Q$ -values by introducing extra four-quark operators with higher derivatives in the lines proposed in refs. [51, 52], but this introduces more unknown couplings and does not address the lack of confinement.

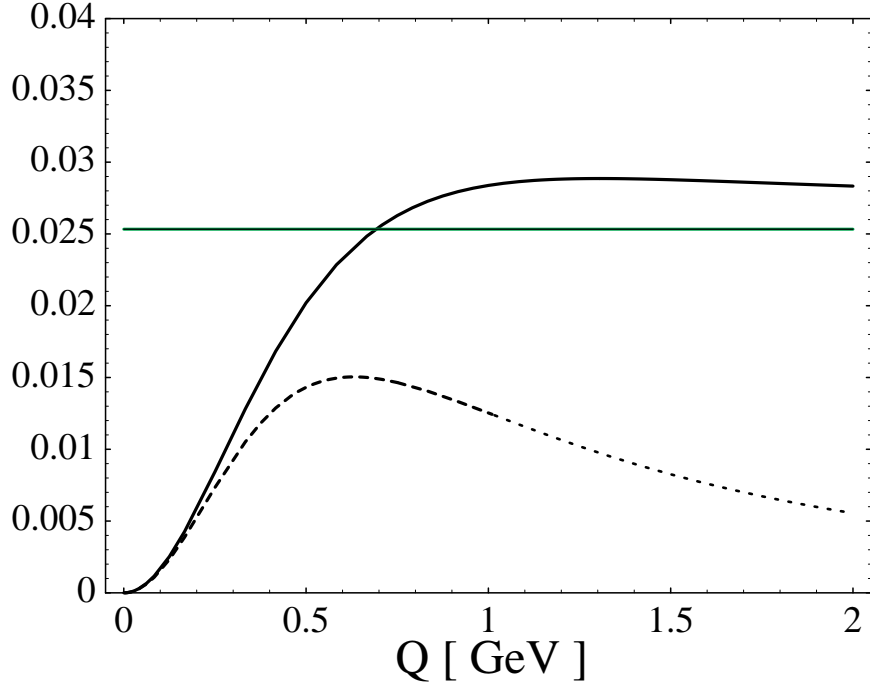


**Fig. 5** The Adler function predicted by the ENJL-Lagrangian in eq. (3.1) (dashed line) compared with the Adler function from the Aleph data (full line).

What is the reason for this failure? In order to find guidance in answering this question, let us compare  $\mathcal{A}_{\text{ENJL}}(Q^2)$  in eq. (3.2) with the expression which results from the LMD approximation to  $\text{QCD}(\infty)$  which we have been advocating in the previous sections, i.e. the approximation where

$$\frac{1}{\pi} \text{Im} \Pi_\infty(t) = 2f_V^2 M_V^2 \delta(t - M_V^2) + \frac{N_c}{16\pi^2} \frac{4}{3} \theta(t - s_0), \quad (3.5)$$

and where for simplicity we are switching off  $\alpha_s$  corrections in the pQCD continuum term. This spectral function produces in the euclidean region the Adler function

$$\mathcal{A}_\infty(Q^2) = -Q^2 \frac{d}{dQ^2} \left( \frac{2f_V^2 M_V^2}{M_V^2 + Q^2} \right) + \frac{N_c}{16\pi^2} \frac{4}{3} \frac{Q^2}{s_0 + Q^2}. \quad (3.6)$$

Clearly eq. (3.6) does not look like eq. (3.2). Even in the region of small  $Q^2$  we see that, firstly, eq. (3.2) lacks  $Q^2/s_0$  contributions<sup>12</sup> that are present in eq. (3.6); and, secondly,

<sup>11</sup> This solves the "paradox" raised in ref. [50]. There is no overlap between the region where the ENJL-Lagrangian is operational and the region covered by the OPE.

<sup>12</sup> We would like to issue a warning message here: the continuum contributes to some of the  $\mathcal{O}(p^6)$  (and higher) couplings of the chiral expansion. Consequently, saturating these coupling constants with only the resonance contribution, as is sometimes done by invoking e.g. VMD arguments, may be misleading.

also the  $Q^2$  dependence of the resonance contribution is misrepresented in eq. (3.2), at least insofar as  $\bar{\Pi}(Q^2)$  is  $Q^2$  dependent. All in all, the low- $Q^2$  dependence of eq. (3.2) appears to be “incorrect” if expected to resemble the one in eq. (3.6) but, as we shall see, in a way that can be amended. The amendment will consist in adding the proper higher dimensional composite operators. We shall see that this addition is nothing but the implementation of the *matching conditions* inherent to any effective Lagrangian construction.

### 3.2 Higher Dimension Operators and Confinement

There will be two distinct classes of higher dimensional operators according to whether they originate from the *continuum* or from the prominent low energy narrow state, which we shall call for short the *resonance*. This is because chiral symmetry is realized differently in these two regions of the spectrum. In the case of the *continuum*, chiral symmetry is manifest by construction and the new higher-dimensional operators to be added to the Lagrangian in eq. (3.1) will contain solely combinations of external fields suppressed by the corresponding powers of  $s_0$ , with chiral symmetry realized in a linear way. A possible example is the operator

$$\frac{1}{s_0} \text{tr} \{ F_{L\mu\nu}(x) \square F_L^{\mu\nu}(x) + F_{R\mu\nu}(x) \square F_R^{\mu\nu}(x) \} . \quad (3.7)$$

On the other hand, operators originating in the contribution from the lowest *resonance* must have spontaneous chiral symmetry breaking built in, and therefore they will appear as chirally symmetric in a nonlinear way; i.e. they will eventually generate effective couplings involving the Nambu–Goldstone bosons encoded in the  $U$ –matrix and suppressed by a characteristic mass scale proportional to the  $Q\bar{Q}$  production threshold  $2M_Q$ . A possible example of an operator of this type is the dimension six operator

$$\frac{1}{4M_Q^2} \text{tr} \left\{ F_{L\mu\nu}(x) U(x)^\dagger [\square F_R^{\mu\nu}(x)] U(x) + F_{R\mu\nu}(x) U(x) [\square F_L^{\mu\nu}(x)] U(x)^\dagger \right\} . \quad (3.8)$$

In order to proceed to the explicit construction of these higher dimension operators it helps to have yet another perspective on the failure of eq. (3.1) to reproduce the expected structure of the LMD approximation to QCD( $\infty$ ) . When computing the imaginary part of  $\Pi_{\text{ENJL}}$  in eq. (3.2) one finds:

$$\frac{1}{\pi} \text{Im} \Pi(t)_{\text{ENJL}} = \frac{\frac{1}{\pi} \text{Im} \bar{\Pi}(t)}{\left(1 - t \frac{8\pi^2 G_V}{N_c \Lambda_\chi^2} \text{Re} \bar{\Pi}(t)\right)^2 + \left(t \frac{8\pi^2 G_V}{N_c \Lambda_\chi^2} \text{Im} \bar{\Pi}(t)\right)^2} . \quad (3.9)$$

The ENJL spectral function has a continuous shape, as shown in Fig. 6, whereas the large- $N_c$  result should be a sum of narrow states; or at least a dominant narrow state as in eq. (3.5).

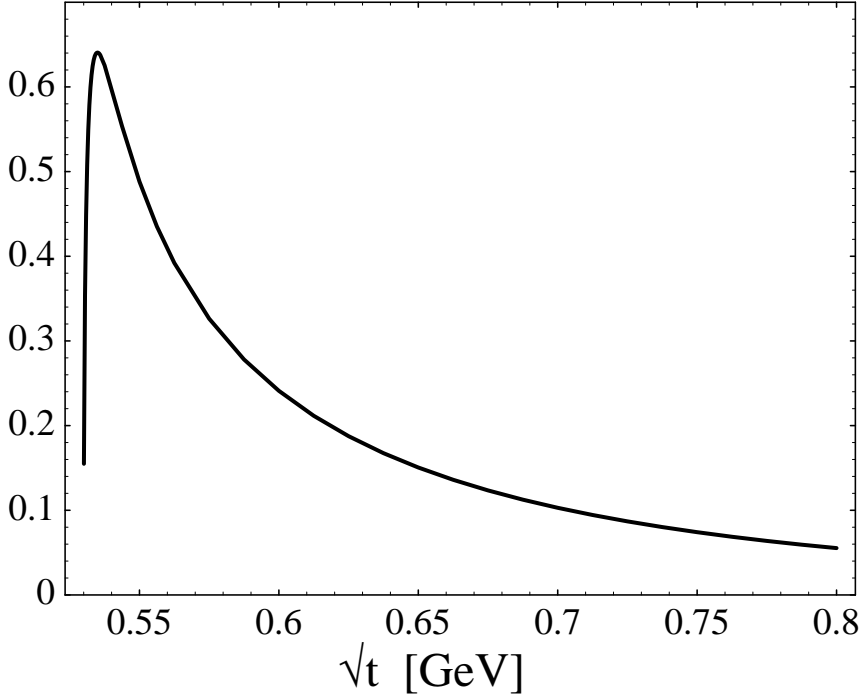


**Fig. 6** The vector spectral function predicted by the ENJL-Lagrangian [24]

The shape in Fig. 6 seems reminiscent of the one corresponding to a “ $\rho$ -resonance” with a “finite width” proportional to

$$\gamma = t \frac{8\pi^2 G_V}{N_c \Lambda_\chi^2} \text{Im}\bar{\Pi}(t), \quad (3.10)$$

and, at first sight, it could even be taken as a success of ENJL. This shape however is more of a *failure* than a success because it involves a “finite width” which is proportional to  $\text{Im}\bar{\Pi}(t)$  and therefore of  $\mathcal{O}(N_c^0)$  while in the large- $N_c$  limit of QCD, which after all  $\mathcal{L}_{\text{ENJL}}$  in eq. (3.1) is supposed to approximate in some way, it should be of  $\mathcal{O}(1/N_c)$ . The wrong large- $N_c$  behaviour of the ENJL width is actually due to the fact that the ENJL spectral function has on-shell  $Q\bar{Q}$  pairs (which involves an extra factor of  $N_c$ ), i.e. precisely to the lack of *confinement*. What is needed here is to find the extra physics which generates the formal limit  $\text{Im}\bar{\Pi}(t) \rightarrow 0$  in a consistent fashion, for then as  $\gamma \rightarrow 0$

$$\lim_{\gamma \rightarrow 0} \frac{\gamma}{\left(1 - t \frac{8\pi^2 G_V}{N_c \Lambda_\chi^2} \text{Re}\bar{\Pi}(t)\right)^2 + \gamma^2} \rightarrow \pi \delta \left(1 - t \frac{8\pi^2 G_V}{N_c \Lambda_\chi^2} \text{Re}\bar{\Pi}(t)\right), \quad (3.11)$$

and the narrow width limit would follow.

The obvious way to perform this limit that comes to one’s mind is to take the limit  $M_Q \rightarrow \infty$ . This is actually what happens in QCD( $\infty$ ) in two dimensions [53, 54], where the mass of the quark is pushed to infinity by the need to regulate the theory in the infrared region; and in two dimensions this is in fact how confinement takes place. Here this does not work because the constituent quark mass  $M_Q$  given by the dynamics of  $\mathcal{L}_{\text{ENJL}}$  in eq. (3.1) is finite. One can nevertheless proceed as follows. Let us consider the very low- $Q^2$  region. Since at  $Q^2 = 0$  the operators of eq. (3.1) produce the right physics, one can start at  $Q^2 = 0$  and work the way up by examining what happens when trying an expansion in powers of

$Q^2/4M_Q^2$ . Because  $M_Q$  is finite, the  $Q^2$  dependence of  $\bar{\Pi}(Q^2)$  is a consequence of the fact that  $\text{Im}\bar{\Pi}(t)$  is nonvanishing. The  $Q^2$  dependence of  $\bar{\Pi}(Q^2)$  originates from the production of constituent  $Q\bar{Q}$ -pairs in the physical spectral function; in other words from the *lack of confinement*. Indeed, the  $Q^2$  dependence is given by the dispersive integral

$$\bar{\Pi}(Q^2) = \bar{\Pi}(0) - Q^2 \int_{4M_Q^2}^{\infty} \frac{dt}{t(t+Q^2)} \frac{1}{\pi} \text{Im}\bar{\Pi}(t), \quad (3.12)$$

where  $\frac{1}{\pi} \text{Im}\bar{\Pi}(t)$  is the spectral function associated with the constituent  $Q\bar{Q}$ -pairs. It is in fact this dispersion relation that holds the key to the remedy we are looking for. The crucial point is that eq. (3.12) shows that  $\bar{\Pi}(Q^2)$  is analytic for  $Q^2 < 4M_Q^2$ . It can be expanded in powers of  $Q^2/4M_Q^2$  and therefore all the “wrong”  $Q^2$  dependence causing trouble can be systematically removed by adding to the Lagrangian in eq. (3.1) an *infinite* set of local operators involving external fields of dimension  $n \geq 6$ :

$$\mathcal{L}_{\text{res}} = \sum_{n=6}^{\infty} c_n \mathcal{O}_n^{\text{res}}. \quad (3.13)$$

The lowest dimension is six because the first operator corresponds to the first derivative of the self-energy function  $\bar{\Pi}(Q^2)$ . The coefficients  $c_n$  in front of these local operators are known since they are adjusted so that all powers of  $Q^2/4M_Q^2$  coming from the Taylor expansion of  $\bar{\Pi}(Q^2)$  cancel out in their contribution to the Adler function in eq. (3.2). For instance an explicit operator of dimension six which removes the “wrong” non-confining dependence of  $\mathcal{O}(Q^2)$  is

$$\mathcal{O}_6 = \bar{\Pi}'(0) \text{ tr} \left\{ U^\dagger (D^\alpha F_R^{\mu\nu}) U (D_\alpha F_{L\mu\nu}) \right\}, \quad (3.14)$$

where as usual the trace is in flavour space, and  $\bar{\Pi}'(0)$  stands for

$$\bar{\Pi}'(0) \equiv \frac{d\bar{\Pi}}{dQ^2}(0) = \frac{-N_c}{16\pi^2 M_Q^2} \frac{4}{15} \Gamma(1, \epsilon). \quad (3.15)$$

The presence of  $\Gamma(1, \epsilon)$  in eq. (3.15) is due to the proper time regularization which we have adopted to define  $\bar{\Pi}(Q^2)$  in eq. (3.3). The “wrong” non-confining  $Q^2$  dependence is regularization dependent and therefore, the counterterms which are added to cancel them will be regularization dependent as well. The net physical effect when the *infinite* set of local operators in eq. (3.13) is added, is formally the same as letting  $M_Q \rightarrow \infty$  in the  $\frac{1}{\pi} \text{Im}\bar{\Pi}(t)$  spectral function, namely  $\bar{\Pi}(Q^2) \rightarrow \bar{\Pi}(0)$ .

### 3.3 Higher Dimension Operators and Matching Conditions

The higher dimension operators in eq. (3.13) can also be viewed as part of the *matching* conditions which are required on the ENJL Lagrangian in eq. (3.1) to become an effective Lagrangian describing a narrow width confined vector state. Indeed, once these operators are included, effectively one is doing the following replacement in eq. (3.2):

$$\Pi_{\text{ENJL}}(Q^2) \rightarrow \bar{\Pi}(0) \sum_{n=0}^{\infty} \left( -Q^2 \frac{8\pi^2 G_V}{N_c \Lambda_\chi^2} \bar{\Pi}(0) \right)^n, \quad (3.16)$$

which is nothing but the expansion around  $Q^2 = 0$  of

$$\Pi_{\text{eff}}(Q^2) = \frac{\bar{\Pi}(0)}{1 + Q^2 \frac{8\pi^2 G_V}{N_c \Lambda_\chi^2} \bar{\Pi}(0)}, \quad (3.17)$$

and has now the form produced by an infinitely narrow state, i.e.

$$\Pi_{\text{eff}}(Q^2) = \int_0^\infty \frac{dt}{t + Q^2} \frac{1}{\pi} \text{Im}\Pi_{\text{eff}}(t), \quad (3.18)$$

with

$$\frac{1}{\pi} \text{Im}\Pi_{\text{eff}}(t) = \frac{N_c \Lambda_\chi^2}{8\pi^2 G_V} \delta(t - N_c \Lambda_\chi^2 (8\pi^2 G_V \bar{\Pi}(0))^{-1}). \quad (3.19)$$

This is precisely the desired result. It leads to a hadronic contribution to the Adler function

$$\mathcal{A}_{\text{eff}}(Q^2) = -Q^2 \frac{d}{dQ^2} \left( \frac{2f_V^2 M_V^2}{M_V^2 + Q^2} \right), \quad (3.20)$$

with

$$2f_V^2 M_V^2 = \frac{N_c \Lambda_\chi^2}{8\pi^2 G_V} \quad \text{and} \quad M_V^2 = N_c \Lambda_\chi^2 (8\pi^2 G_V \bar{\Pi}(0))^{-1}; \quad (3.21)$$

i.e., the same contribution as the LMD approximation to  $\text{QCD}(\infty)$  formulated in eq. (3.6).

At this point the reader may perhaps wonder about what all this improvement on ENJL has really brought us since it looks as if all we have accomplished is to reproduce eqs. (3.5) and (3.6), which after all we already knew from large- $N_c$  QCD arguments in the first place. The point, as we shall further develop in the next sections, is that imposing that the low-energy physics be governed by the effective Lagrangian in eq. (3.1) with the *infinite* set of *matching* operators of higher dimension understood, constrains the parameters of the dominant low-energy states, which would otherwise be arbitrary. It relates, in particular, the lowest vector state to the lowest axial-vector state in a way which we will describe next.

## 4 The Axial–Vector Channel

We shall now be concerned with two-point functions

$$\Pi_{\mu\nu}^A(q)_{ab} = i \int d^4x e^{iq \cdot x} < 0|T\{A_\mu^a(x) A_\nu^b(0)\}|0> \quad (4.1)$$

of axial–vector quark currents

$$A_\mu^a(x) = \bar{q}(x) \gamma_\mu \gamma_5 \frac{\lambda^a}{\sqrt{2}} q(x), \quad (4.2)$$

where  $\lambda^a$ , as before in eq. (2.2), are Gell-Mann matrices acting on the flavour triplet of  $u$ ,  $d$ ,  $s$  light quarks. In the chiral limit where the light quark masses are set to zero, these two–point functions depend only on one invariant function ( $Q^2 = -q^2 \geq 0$  for  $q^2$  spacelike)

$$\Pi_{\mu\nu}^A(q)_{ab} = (q_\mu q_\nu - g_{\mu\nu} q^2) \Pi_A(Q^2) \delta_{ab}. \quad (4.3)$$

The axial–vector two–point functions predicted by the ENJL Lagrangian have been discussed in ref. [24]. The self–energy function  $\Pi_A(Q^2)$  has the following form

$$\Pi_A(Q^2) = \frac{\bar{\Pi}_A(Q^2)}{1 + Q^2 \frac{8\pi^2 G_V}{N_c \Lambda_\chi^2} \bar{\Pi}_A(Q^2)}, \quad (4.4)$$

where  $\bar{\Pi}_A(Q^2)$  is now given by

$$\bar{\Pi}_A(Q^2) = \bar{\Pi}(Q^2) + \frac{f^2(Q^2)}{Q^2}, \quad (4.5)$$

with  $\bar{\Pi}(Q^2)$  the same function as the one defined in eq. (3.3) and

$$f^2(Q^2) = \frac{N_c}{16\pi^2} 8M_Q^2 \int_0^1 dx \Gamma(0, x_Q). \quad (4.6)$$

It is convenient to introduce the function

$$g_A(Q^2) = \frac{1}{1 + (G_V/\Lambda_\chi^2) 4M_Q^2 \int_0^1 dx \Gamma(0, x_Q)}, \quad (4.7)$$

and then rewrite  $\Pi_A(Q^2)$  as follows

$$\Pi_A(Q^2) = \frac{\bar{\Pi}(Q^2) g_A^2(Q^2)}{1 + Q^2 \frac{8\pi^2 G_V}{N_c \Lambda_\chi^2} \bar{\Pi}(Q^2) g_A(Q^2)} + \frac{f^2(Q^2) g_A(Q^2)}{Q^2}. \quad (4.8)$$

As in the case of the vector channel one notices that eq. (4.8) could match onto an axial Adler function

$$\mathcal{A}_A(Q^2) = -Q^2 \frac{d}{dQ^2} \left( \frac{2f_\pi^2}{Q^2} + \frac{2f_A^2 M_A^2}{M_A^2 + Q^2} \right) + \frac{N_c}{16\pi^2} \frac{4}{3} \frac{Q^2}{s_0 + Q^2}, \quad (4.9)$$

generated by a narrow width spectral function corresponding to the LMD approximation in QCD( $\infty$ ) i.e.,

$$\frac{1}{\pi} \text{Im} \Pi_A(t) = 2f_\pi^2 \delta(t) + 2f_A^2 M_A^2 \delta(t - M_A^2) + \frac{N_c}{16\pi^2} \frac{4}{3} \theta(t - s_0), \quad (4.10)$$

provided that both  $\bar{\Pi}(Q^2)$  and  $f^2(Q^2)$  get their  $Q^2$  dependence, induced by  $Q\bar{Q}$  discontinuities, canceled by the inclusion of appropriate higher dimensional composite operators in the external fields.

We emphasize that the procedure of introducing an infinite number of local operators adds no unknown parameters, as the coefficients accompanying the operators are fixed by the coefficients of the Taylor expansion at zero momentum of the functions  $\bar{\Pi}(Q^2)$  and  $f^2(Q^2)$  which are explicitly known. Furthermore, one also has to add the operators that fix the contribution of the continuum, as was explained in the case of the vector channel in subsec. 3.2. Once this is implemented the masses and coupling constants of the dominant low–energy states in the vector and axial–vector channels are completely fixed in terms of the parameters  $G_S, G_V$  and  $\Lambda_\chi$  in a way which we summarize below.

i) THE GAP EQUATION.

The gap equation in eq. (3.4) relates  $G_S$  to the ratio of the constituent quark mass  $M_Q$  and the scale  $\Lambda_\chi$

$$\frac{1}{G_S} = \epsilon \Gamma(-1, \epsilon), \quad \text{with} \quad \epsilon \equiv \frac{M_Q^2}{\Lambda_\chi^2}. \quad (4.11)$$

ii) THE COUPLING CONSTANT  $g_A$ .

The coupling constant  $g_A$  is governed by the size of the  $G_V$  coupling

$$g_A \equiv g_A(0) = (1 + 4G_V \epsilon \Gamma(0, \epsilon))^{-1}. \quad (4.12)$$

iii) MASSES.

The masses of the vector and axial–vector states are then fixed as follows

$$M_V^2 = \frac{3}{2} \frac{\Lambda_\chi^2}{G_V \Gamma(0, \epsilon)} \frac{1}{1 - g_A} = 6M_Q^2 \frac{g_A}{1 - g_A}, \quad \text{and} \quad M_A^2 = \frac{M_V^2}{g_A}. \quad (4.13)$$

iv) THE COUPLING CONSTANTS.

The coupling constants of the lowest narrow states are then also fixed:

$$f_\pi^2 = \frac{N_c}{16\pi^2} 4M_Q^2 g_A \Gamma(0, \epsilon), \quad (4.14)$$

$$f_V^2 = \frac{N_c}{16\pi^2} \frac{2}{3} \Gamma(0, \epsilon), \quad (4.15)$$

$$f_A^2 = g_A^2 f_V^2. \quad (4.16)$$

With these results, the 1st and 2nd Weinberg sum rules, which in the case of LMD imply the well known relations

$$f_\pi^2 + f_A^2 M_A^2 = f_V^2 M_V^2, \quad (4.17)$$

$$f_A^2 M_A^4 = f_V^2 M_V^4, \quad (4.18)$$

are then automatically satisfied. It appears then, that just removing the *non-confining* terms in the vector and axial–vector two–point functions predicted by the usual ENJL–Lagrangian guarantees their correct *matching* to the QCD short–distance behaviour. This shows, in retrospect, that the choice of an initial ENJL–*ansatz* as a starting effective Lagrangian was quite a good one. However, as we shall later see, the removal of the *non-confining* contributions in Green’s functions beyond two–point functions is not enough to guarantee, in general, the correct *matching* to the QCD short–distance behaviour and further local operators have to be introduced.

## 4.1 The Electromagnetic $\pi^+ - \pi^0$ Mass–Difference

In the chiral limit, and in the presence of electromagnetic interactions to lowest order in the fine structure constant  $\alpha$ , the hadronic spectral functions in eqs. (3.5) and (4.10) induce an

electromagnetic mass for the charged pion, which is finite when the spectral functions obey the 1st and 2nd Weinberg sum rules<sup>13</sup>. This results in the expression

$$m_{\pi^+}^2|_{\text{EM}} = \frac{\alpha}{\pi} \frac{3}{4} \frac{M_A^2 M_V^2}{M_A^2 - M_V^2} \log \frac{M_A^2}{M_V^2}, \quad (4.19)$$

which in terms of the parameters  $M_Q$  and  $g_A$  defined above reads

$$m_{\pi^+}^2|_{\text{EM}} = \frac{\alpha}{\pi} \frac{9}{2} M_Q^2 \frac{g_A}{(1 - g_A)^2} \log \frac{1}{g_A}. \quad (4.20)$$

We show below in Fig. 7 a two-dimensional plot of the resulting electromagnetic pion mass difference  $\Delta m_\pi \equiv m_{\pi^+} - m_{\pi^0}$  as a function of  $M_Q$  and  $g_A$  when these parameters are varied in the ranges  $200 \text{ MeV} \leq M_Q \leq 400 \text{ MeV}$  and  $0.4 \leq g_A \leq 0.6$ . Experimentally [55],  $\Delta m_\pi = (4.5936 \pm 0.0005) \text{ MeV}$ . This corresponds to the *plateau* shown in Fig. 7. The intersection of eq. (4.20) with this *plateau* results in a line which correlates  $M_Q$  and  $g_A$ . The figure shows that a very reasonable choice of values for these two parameters can reproduce the experimental result. We shall be more precise about the values of these parameters in subsection 5.2

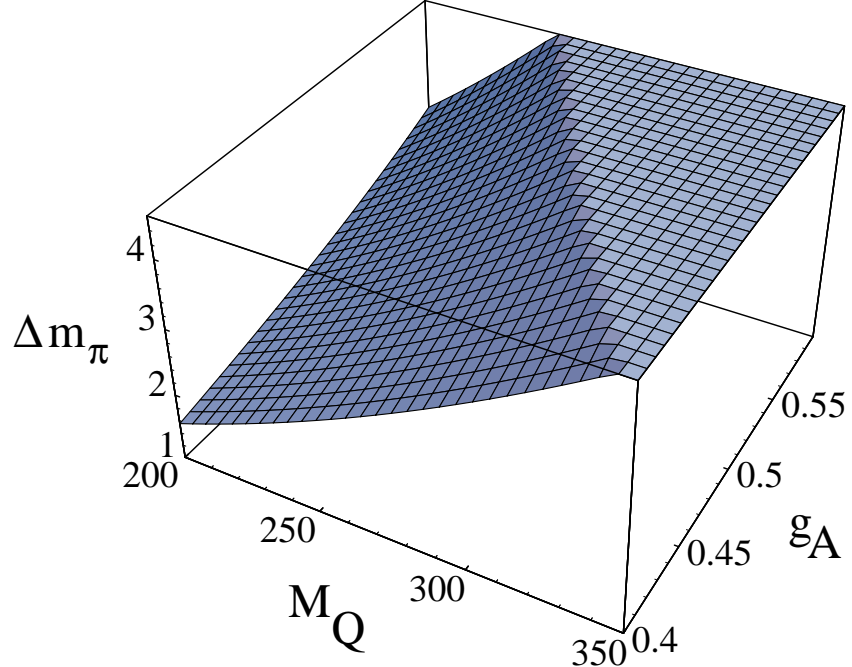


**Fig. 7** The electromagnetic pion mass difference  $\Delta m_\pi$  in MeV versus  $g_A$  and  $M_Q$  (MeV)

## 5 The Low-Energy Effective Lagrangian

The degrees of freedom of the resulting effective low-energy Lagrangian are a pseudoscalar Goldstone field matrix, a vector field matrix  $V(x)$ , a scalar field matrix  $S(x)$ , and an axial-vector field matrix  $A(x)$ . They correspond, therefore, to the wanted LMD spectrum of  $0^-, 1^-$ ,

<sup>13</sup> For an introduction to this subject, see e.g. the lectures in ref. [42], where references to the earlier work are also given.

$0^+$ , and  $1^+$  hadronic states. We postpone the technical discussion concerning the removal of  $Q\bar{Q}$  discontinuities in Green's functions with external scalar sources to another paper. Here, we shall limit ourselves to quote the results we obtain for the effective  $\mathcal{O}(p^4)$  chiral Lagrangian of the Goldstone modes after integrating out the physical scalar fields. It is this dynamical effect which produces the  $L_5$  and  $L_8$  couplings as well as part of the  $\tilde{L}_3$  coupling which we give below. The remaining interactions between the pseudoscalar Goldstone field matrix and the vector and axial–vector field matrices produce the rest of the couplings in the following effective Lagrangian, valid up to  $\mathcal{O}(p^4)$  and also for some of the higher order terms,

$$\begin{aligned}
\tilde{\mathcal{L}}_{\text{eff}} = & \frac{1}{4}f_\pi^2 \left[ \text{tr} \left( D_\mu U D^\mu U^\dagger \right) + \text{tr} \left( \chi U^\dagger + U^\dagger \chi \right) \right] + e^2 C \text{tr} (Q_R U Q_L U^\dagger) \\
& - \frac{1}{4} \text{tr} [V_{\mu\nu} V^{\mu\nu} - 2M_V^2 V_\mu V^\mu] \\
& - \frac{1}{4} \text{tr} [A_{\mu\nu} A^{\mu\nu} - 2M_A^2 A_\mu A^\mu] \\
& - \frac{1}{2\sqrt{2}} [f_V \text{tr} (V_{\mu\nu} f_+^{\mu\nu}) + i\tilde{g}_V \text{tr} (V_{\mu\nu} [\xi^\mu, \xi^\nu]) + f_A \text{tr} (A_{\mu\nu} f_-^{\mu\nu})] \\
& + \tilde{L}_1 \left( \text{tr} D_\mu U^\dagger D^\mu U \right)^2 + 2\tilde{L}_1 \text{tr} (D_\mu U^\dagger D_\nu U \text{tr} D^\mu U^\dagger D^\nu U) \\
& + \tilde{L}_3 \text{tr} (D_\mu U^\dagger D^\mu U D_\nu U^\dagger D^\nu U) \\
& + L_5 \text{tr} [D_\mu U^\dagger D^\mu U (\chi^\dagger U + U^\dagger \chi)] + L_8 \text{tr} (\chi^\dagger U \chi^\dagger U + \chi U^\dagger \chi U^\dagger) \\
& - i\tilde{L}_9 \text{tr} (F_R^{\mu\nu} D_\mu U D_\nu U^\dagger + F_L^{\mu\nu} D_\mu U^\dagger D_\nu U) + L_{10} \text{tr} (U^\dagger F_R^{\mu\nu} U F_{L\mu\nu}) \\
& + H_1 \text{tr} (F_R^{\mu\nu} F_{R\mu\nu} + F_L^{\mu\nu} F_{L\mu\nu}) + H_2 \text{tr} (\chi^\dagger \chi). \tag{5.1}
\end{aligned}$$

Here,

$$V^{\mu\nu} = \nabla^\mu V^\nu - \nabla^\nu V^\mu, \quad A^{\mu\nu} = \nabla^\mu A^\nu - \nabla^\nu A^\mu; \tag{5.2}$$

with  $\nabla$  the covariant derivative defined as

$$\nabla_\mu R \equiv \partial_\mu R + [\Gamma_\mu, R], \tag{5.3}$$

and  $\Gamma_\mu$  the connection

$$\Gamma_\mu = \frac{1}{2} \left\{ \xi^\dagger [\partial_\mu - i(v_\mu + a_\mu)] \xi + \xi [\partial_\mu - i(v_\mu - a_\mu)] \xi^\dagger \right\}. \tag{5.4}$$

We recall that  $v_\mu$  and  $a_\mu$  are external vector and axial–vector matrix field sources, (not to be confused with the hadronic matrix fields  $V_\mu$  and  $A_\mu$ ), and  $F_L^{\mu\nu}$  and  $F_R^{\mu\nu}$  are the external field strength matrix tensors associated with the  $l_\mu = v_\mu - a_\mu$  and  $r_\mu = v_\mu + a_\mu$  sources. We are also using the notation  $U = \xi \xi^\dagger$  with

$$f_\pm^{\mu\nu} = \xi F_L^{\mu\nu} \xi^\dagger \pm \xi^\dagger F_R^{\mu\nu} \xi \quad \text{and} \quad \xi_\mu = i\xi^\dagger D_\mu U \xi^\dagger. \tag{5.5}$$

This is the effective Lagrangian which results from the ENJL–ansatz after removal of *non-confining*  $Q\bar{Q}$  discontinuities. As already mentioned, this guarantees the correct *matching* to the QCD short–distance behaviour for two–point functions only. The couplings  $\tilde{g}_V$ ,  $\tilde{L}_9$ , and  $\tilde{L}_1$ ,  $\tilde{L}_3$  are correlated with three– and four–point functions which still require the introduction of extra higher dimension operators to guarantee the correct *matching* to the leading QCD

short-distance behaviour. This is why we put a *tilde* on them, and we shall discuss how they have to be modified in the next subsection. All the constants appearing in the Lagrangian in eq. (5.1) are functions of  $G_S$ ,  $G_V$ , and  $\Lambda_\chi$  alone or equivalently  $g_A$ ,  $M_Q$  and  $\Gamma_0 \equiv \Gamma(0, \epsilon)$ . The masses  $M_V^2$  and  $M_A^2$  have already been given in eq. (4.13), and the couplings  $f_\pi^2$ ,  $f_V^2$  and  $f_A^2$  in eqs. (4.14), (4.15) and (4.16). The constant  $C$  is related to the electromagnetic  $\pi^+ - \pi^0$  mass difference in eq. (4.20),

$$\frac{2e^2 C}{f_\pi^2} = m_{\pi^+}^2|_{\text{EM}}. \quad (5.6)$$

One could in principle consider as well terms of  $\mathcal{O}(e^2 p^2)$  but this goes beyond the scope of this paper. At this stage i.e., after removing  $Q\bar{Q}$  discontinuities in the initial ENJL-*ansatz*, the result for the VPP coupling  $\tilde{g}_V$  is

$$\tilde{g}_V^2 = \frac{N_c}{16\pi^2} \frac{1}{6} (1 - g_A^2)^2 \Gamma_0, \quad (5.7)$$

and the results for the other couplings in eq.(5.1) are:

$$\tilde{L}_1 = \frac{N_c}{16\pi^2} \frac{1}{48} (1 - g_A^2)^2 \Gamma_0, \quad (5.8)$$

$$\tilde{L}_3 = \frac{N_c}{16\pi^2} \frac{1}{8} \left[ -(1 - g_A^2)^2 + 2g_A^4 \right] \Gamma_0, \quad (5.9)$$

$$L_5 = \frac{N_c}{16\pi^2} \frac{1}{4} g_A^3 \Gamma_0, \quad (5.10)$$

$$L_8 = \frac{N_c}{16\pi^2} \frac{1}{16} g_A^2 \Gamma_0, \quad (5.11)$$

$$\tilde{L}_9 = \frac{N_c}{16\pi^2} \frac{1}{6} (1 - g_A^2) \Gamma_0, \quad (5.12)$$

$$L_{10} = \frac{N_c}{16\pi^2} \frac{-1}{6} (1 - g_A^2) \Gamma_0. \quad (5.13)$$

Integrating out the vector and axial-vector fields in the Lagrangian of eq. (5.1) produces terms of  $\mathcal{O}(p^6)$ . However, to that order, there are two extra sources of other possible contributions which must be taken into account. One is the effect of integrating out the vector and axial-vector fields in the other  $\mathcal{O}(p^3)$  interaction terms which are not included in  $\mathcal{L}_{\text{eff}}$  in eq. (5.1), (terms like e.g.  $\epsilon_{\mu\nu\rho\sigma} \text{tr}(V^\mu \xi^\nu \xi^\rho \xi^\sigma)$ ); the other source, as already mentioned, is the effect of new operators coming from the *matching* of Green's functions beyond two-point functions to short-distance QCD.

The Adler two-point functions which we have discussed in the previous sections, i.e. the expressions in eqs. (3.6) and (4.9) with the masses and couplings as given in eqs. (4.13) and (4.14), (4.15), (4.16), are the result of the full resummation of all the relevant terms in the effective Lagrangian. Expanding these Adler functions in powers of  $Q^2$  is, of course, another way of obtaining the couplings of the corresponding operators in the effective Lagrangian which govern the behaviour of these functions.

## 5.1 Dynamical Symmetries of the Low-Energy Effective Lagrangian

The results we find at this level for the low-energy couplings show already a lot of interesting symmetries. It is worthwhile describing them and comparing them with the dynamical relations discussed in ref. [27]. For the sake of comparison it is more convenient to rewrite the

results we have found for the couplings  $f_V$ ,  $f_A$  and  $\tilde{g}_V$  in the following way

$$f_V = \sqrt{\frac{1}{1-g_A}} \frac{f_\pi}{M_V}, \quad (5.14)$$

$$f_A = g_A \sqrt{\frac{1}{1-g_A}} \frac{f_\pi}{M_V}, \quad (5.15)$$

$$\tilde{g}_V = \frac{1+g_A}{2} \sqrt{1-g_A} \frac{f_\pi}{M_V}. \quad (5.16)$$

The results for the couplings in eqs. (5.8) to (5.13) can then be written as follows:

$$\tilde{L}_1 = \frac{1}{8} \tilde{g}_V^2, \quad (5.17)$$

$$\tilde{L}_3 = -6\tilde{L}_1 + g_A L_5, \quad (5.18)$$

$$L_5 = 4g_A L_8, \quad (5.19)$$

$$L_8 = \frac{N_c}{16\pi^2} \frac{1}{16} g_A^2 \Gamma_0, \quad (5.20)$$

$$\tilde{L}_9 = \frac{1}{2} f_V \tilde{g}_V, \quad (5.21)$$

$$L_{10} = \frac{-1}{4} (f_V^2 - f_A^2). \quad (5.22)$$

Some of the relations encoded in the Lagrangian (5.1) turn out to be common to those discussed in ref. [27] in connection with the formulation of chiral Lagrangians of vector and axial–vector mesons obeying short–distance QCD constraints. They are the following:

- The 1st and 2nd Weinberg sum rules in eqs.(4.17) and (4.18).
- The relationship between the constant  $L_{10}$  and the  $f_V$  and  $f_A$  couplings in eq.(5.22).
- The relationship between the constant  $\tilde{L}_9$  and the  $f_V$  and  $\tilde{g}_V$  couplings in eq.(5.21).
- The relations:

$$\tilde{L}_1 = \frac{1}{8} \tilde{g}_V^2, \quad \text{and} \quad \tilde{L}_3|_{\text{vector}} = -6\tilde{L}_1, \quad (5.23)$$

where  $\tilde{L}_3|_{\text{vector}}$  means the contribution induced by vector exchange to  $\tilde{L}_3$ . In ref. [27] it is shown that these two relations follow from the assumption that the forward scattering amplitudes of two pseudoscalar mesons obey the Froissart bound [56, 57].

The fact that the effective Lagrangian in (5.1) obeys automatically these relations shows again that the ENJL–Lagrangian *ansatz* plus the corresponding set of local operators required to remove the non–confining  $Q\bar{Q}$ –discontinuities which it generates is already a very good effective Lagrangian to describe the LMD approximation to  $\text{QCD}(\infty)$ . There are however other relations in ref. [27] which the effective Lagrangian in (5.1) does not quite satisfy. Let us describe them.

- i) In ref. [27] it is shown that the assumption that the pion electromagnetic form factor  $F(q^2)$  with the charge normalization condition  $F(0) = 1$ , obeys an unsubtracted dispersion

relation, and the saturation of the dispersive integral with just the  $\rho$ -pole leads to the relation

$$f_V g_V \frac{M_V^2}{f_\pi^2} = 1, \quad (5.24)$$

with  $g_V$  the physical  $\rho\pi\pi$  coupling constant.

ii) A similar assumption of an unsubtracted dispersion relation for the axial form factor in  $\pi \rightarrow e\nu_e\gamma$ , with the same saturation assumption of the dispersive integral by a resonance pole was shown in [27] to lead to the relation

$$f_V = 2g_V, \quad (5.25)$$

which is sometimes called the KSFR-relation [58, 59].

The combination of i) and ii) results in

$$f_V = 2g_V = \sqrt{2} \frac{f_\pi}{M_V}. \quad (5.26)$$

The combination of i), ii) and the two Weinberg sum rules in eqs.(4.17) and (4.18) imply

$$M_A = \sqrt{2}M_V \quad (5.27)$$

and therefore

$$(\pi_+^2 - \pi_0^2)_{\text{EM}} = \frac{\alpha}{\pi} \frac{3}{2} M_V^2 \log 2. \quad (5.28)$$

With  $f_\pi$  and  $M_V$  as independent variables, the other couplings are then all fixed:

$$f_V = \sqrt{2} \frac{f_\pi}{M_V}, \quad g_V = \frac{1}{\sqrt{2}} \frac{f_\pi}{M_V}, \quad \text{and} \quad f_A = \frac{f_\pi}{M_A}. \quad (5.29)$$

When compared to the results in eqs. (5.14), (5.16) and (5.15) it looks as if there is no unique solution for  $g_A$  which can reproduce all these constraints simultaneously. The value  $g_A = \frac{1}{2}$  reproduces the result  $M_A = \sqrt{2}M_V$  and the couplings for  $f_V$  and  $f_A$  in eq. (5.29), but not  $g_V$ . On the other hand, the electromagnetic pion form factor constraint in eq. (5.24) can only be satisfied if  $g_A = 1$ , while the axial-form factor constraint in eq. (5.25) requires  $g_A = 0$ ; but both these two extreme values are excluded by general large- $N_c$  arguments [19].

From the description above, there follows that the question of whether or not the electromagnetic pion form factor and the axial form factor in  $\pi \rightarrow e\nu_e\gamma$  obey unsubtracted dispersion relations is an important issue. In QCD it is indeed expected that these form factors do obey unsubtracted dispersion relations, and there is no reason that the restriction of full QCD to QCD( $\infty$ ) with LMD spoils this property <sup>14</sup>. Let us then consider the electromagnetic pion form factor  $F(Q^2)$  in somewhat more detail. The effective Lagrangian in eq. (5.1) gives:

$$\tilde{F}(Q^2) = 1 - 2\tilde{L}_9 \frac{M_V^2}{f_\pi^2} \frac{Q^2}{M_V^2} + f_V \tilde{g}_V \frac{M_V^2}{f_\pi^2} \frac{Q^2}{M_V^2} \frac{Q^2}{M_V^2 + Q^2}. \quad (5.30)$$

---

<sup>14</sup> Short-distance QCD arguments for a  $1/Q^2$  fall-off of the electromagnetic pion form factor can be found in ref. [60]. The  $1/Q^2$  fall-off also follows rigorously from an analysis [26] of QCD short-distance constraints on three-point functions saturated by a vector state and pseudoscalar Goldstones only.

The first term 1 is the  $\mathcal{O}(p^2)$  contribution; the second term comes from the  $\tilde{L}_9$ -coupling; the last one from integrating out the vector field  $V$  from the  $\mathcal{O}(p^3)$  interaction terms. Recall that  $\tilde{L}_9 = \frac{1}{2}f_V\tilde{g}_V$ , with  $f_V$  and  $\tilde{g}_V$  defined in eqs. (5.13) and (5.14). Clearly,

$$\tilde{F}(Q^2) = 1 - f_V\tilde{g}_V \frac{M_V^2}{f_\pi^2} \frac{Q^2}{M_V^2} \left(1 - \frac{Q^2}{M_V^2 + Q^2}\right) \quad (5.31)$$

$$= 1 - \frac{1+g_A}{2} \frac{Q^2}{M_V^2 + Q^2}. \quad (5.32)$$

The problem with this form factor is that it does not satisfy the QCD requirement that asymptotically in  $Q^2$  it should fall as  $\frac{1}{Q^2}$ . It does not have either the expected LMD behaviour

$$F(Q^2) = \frac{M_V^2}{M_V^2 + Q^2}. \quad (5.33)$$

Notice that here we are talking about an on-shell form factor (the pions are on-shell), and its imaginary part is supposed to have one state only, the lowest vector meson state. There is no perturbative on-shell continuum here. In order to implement the correct large- $Q^2$  behaviour we are then forced -once more- to introduce a set of an infinite number of local operators in external fields. These are operators of the *second class type* discussed in section 3.2. Their contribution to  $F(Q^2)$ , let us call it  $\tilde{f}(Q^2)$ , when re-summed must give:

$$\tilde{f}(Q^2) = -\frac{1-g_A}{2} \left\{ \frac{Q^2}{M_V^2} - \frac{Q^4}{M_V^2(M_V^2 + Q^2)} \right\}, \quad (5.34)$$

for then, the overall form factor will be

$$F(Q^2) = 1 - \frac{1+g_A}{2} \frac{Q^2}{M_V^2 + Q^2} - \frac{1-g_A}{2} \frac{Q^2}{M_V^2 + Q^2} = \frac{M_V^2}{M_V^2 + Q^2}, \quad (5.35)$$

as wanted. The overall effect of this infinite number of local operators is a simultaneous modification of the coupling constant  $\tilde{g}_V$  and the constant  $\tilde{L}_9$  in the effective Lagrangian in (5.1) as follows:

$$\tilde{g}_V = \frac{1+g_A}{2} \sqrt{1-g_A} \frac{f_\pi}{M_V} \rightarrow \left( \frac{1+g_A}{2} + \frac{1-g_A}{2} \right) \sqrt{1-g_A} \frac{f_\pi}{M_V} \quad (5.36)$$

$$= \sqrt{1-g_A} \frac{f_\pi}{M_V} \equiv g_V, \quad (5.37)$$

and

$$\tilde{L}_9 = \frac{N_c}{16\pi^2} \frac{1}{6} (1-g_A^2) \Gamma_0 \rightarrow \frac{N_c}{16\pi^2} \frac{1}{3} (1-g_A) \Gamma_0 \equiv L_9. \quad (5.38)$$

A similar modification of the coupling constants  $\tilde{L}_1, \tilde{L}_3$  also has to be made, accordingly, so as to preserve the relations in eq. (5.23) which ensure the short-distance *matching* for four-point functions, with the result

$$\tilde{L}_1 = \frac{N_c}{16\pi^2} \frac{1}{48} (1-g_A^2)^2 \Gamma_0 \rightarrow \frac{N_c}{16\pi^2} \frac{1}{12} (1-g_A)^2 \Gamma_0 \equiv L_1, \quad (5.39)$$

$$\tilde{L}_3 = -6\tilde{L}_1 + g_A L_5 \rightarrow -6L_1 + g_A L_5 \equiv L_3. \quad (5.40)$$

The new coupling constants preserve the symmetries

$$L_1 = \frac{1}{8}g_V^2, \quad (5.41)$$

$$L_3 = -6L_1 + g_A L_5, \quad (5.42)$$

$$L_9 = \frac{1}{2}f_V g_V, \quad (5.43)$$

and, now, they also satisfy the relation

$$f_V g_V = \frac{f_\pi^2}{M_V^2}. \quad (5.44)$$

Let us next consider the axial form factor  $G_A(Q^2)$  in  $\pi \rightarrow e\nu\gamma$ . Again, the condition of saturation of the imaginary part with one axial–vector state, and no subtractions in the dispersion relation implies [27]:  $2f_V g_V - f_V^2 = 0$ . It turns out that now, using eqs. (5.14) and (5.44), there is indeed a solution which satisfies this constraint, namely:

$$g_A = \frac{1}{2}. \quad (5.45)$$

The net effect is that the number of independent input parameters has now been reduced from three to two.

## 5.2 The LMD Effective Lagrangian of Large- $N_c$ QCD

We finally find that after correcting the initial ENJL–Lagrangian *ansatz* for the unwanted non–confining  $Q\bar{Q}$ –discontinuities and demanding the correct *matching* between the leading QCD short–distance behaviour of the VPP and PVA three–point functions and the asymptotic behaviour of the corresponding hadronic form factors, the resulting low–energy effective Lagrangian which describes LMD in  $\text{QCD}(\infty)$ , to  $\mathcal{O}(p^4)$  in the chiral expansion, has the simple form

$$\begin{aligned} \mathcal{L}_{\text{eff}} = & \frac{1}{4}f_\pi^2 \left[ \text{tr} \left( D_\mu U D^\mu U^\dagger \right) + \text{tr} \left( \chi U^\dagger + U^\dagger \chi \right) \right] + e^2 C \text{tr} (Q_R U Q_L U^\dagger) \\ & - \frac{1}{4} \text{tr} [V_{\mu\nu} V^{\mu\nu} - 2M_V^2 V_\mu V^\mu] \\ & - \frac{1}{4} \text{tr} [A_{\mu\nu} A^{\mu\nu} - 4M_V^2 A_\mu A^\mu] \\ & - \frac{1}{4} \frac{f_\pi}{M_V} \text{tr} (2V_{\mu\nu} f_+^{\mu\nu} + iV_{\mu\nu} [\xi^\mu, \xi^\nu] + A_{\mu\nu} f_-^{\mu\nu}) \\ & + L_1 \left( \text{tr} D_\mu U^\dagger D^\mu U \right)^2 + 2L_1 \text{tr} \left( D_\mu U^\dagger D_\nu U \text{tr} D^\mu U^\dagger D^\nu U \right) \\ & + L_3 \text{tr} \left( D_\mu U^\dagger D^\mu U D_\nu U^\dagger D^\nu U \right) \\ & + L_5 \text{tr} \left[ D_\mu U^\dagger D^\mu U \left( \chi^\dagger U + U^\dagger \chi \right) \right] + L_8 \text{tr} \left( \chi^\dagger U \chi^\dagger U + \chi U^\dagger \chi U^\dagger \right) \\ & - iL_9 \text{tr} \left( F_R^{\mu\nu} D_\mu U D_\nu U^\dagger + F_L^{\mu\nu} D_\mu U^\dagger D_\nu U \right) + L_{10} \text{tr} \left( U^\dagger F_R^{\mu\nu} U F_{L\mu\nu} \right) \\ & + H_1 \text{tr} (F_R^{\mu\nu} F_{R\mu\nu} + F_L^{\mu\nu} F_{L\mu\nu}) + H_2 \text{tr} (\chi^\dagger \chi), \end{aligned} \quad (5.46)$$

with, so far, two free parameters  $M_Q$  and  $\Gamma_0$  which are such that:

$$f_\pi^2 = \frac{N_c}{16\pi^2} 2M_Q^2 \Gamma_0 \quad \text{and} \quad M_V^2 = \frac{1}{2} M_A^2 = 6M_Q^2. \quad (5.47)$$

The constant  $C$  is then fixed,

$$\frac{2e^2 C}{f_\pi^2} = \frac{\alpha}{\pi} 9M_Q^2 \log 2, \quad (5.48)$$

and the Gasser–Leutwyler  $L_i$  constants are all proportional to  $\frac{N_c}{16\pi^2} \Gamma_0$ , i.e. to  $3\frac{f_\pi^2}{M_V^2}$ :

$$6L_1 = 3L_2 = \frac{-8}{7}L_3 = 4L_5 = 8L_8 = \frac{3}{4}L_9 = -L_{10} = \frac{N_c}{16\pi^2} \frac{1}{8} \Gamma_0. \quad (5.49)$$

Notice that the dependence on the regularization chosen in the ENJL–*ansatz* only appears as an undetermined overall constant  $\Gamma_0$ . Different regularizations will give different “expressions” for  $\Gamma_0$ , but once the value of  $\Gamma_0$  is traded for a physical observable, all the predictions are regularization independent.

When restricted to the vector and axial–vector sector, the Lagrangian in (5.46) is entirely analogous to the phenomenological Lagrangians discussed in ref. [27]. They are just different formulations of the same physics which describes the LMD of the  $0^-$ ,  $1^-$  and  $1^+$  hadronic states in  $\text{QCD}(\infty)$ . The predictive power of the low–energy effective Lagrangian in (5.46), as compared to various phenomenologically inspired Lagrangian formulations of resonances discussed e.g. in refs. [28–31] and references therein lies in the fact that in our case the vector, axial–vector and scalar couplings are all correlated by one mass scale  $M_Q$  and one dimensionless parameter  $\Gamma_0$ , which can be traded for  $f_\pi$  and  $M_V$ . In order to predict the  $\mathcal{O}(p^4)$   $L_i$ –constants e.g., the phenomenological approaches require  $f_\pi$ ,  $M_V$ , the scalar couplings [28]  $c_m$ ,  $c_d$ , and  $M_S$  as a minimum of input parameters. Going from  $\mathcal{O}(p^4)$  to  $\mathcal{O}(p^6)$  in a phenomenological approach requires many more new input parameters, while in our case they are all fixed by the same  $M_Q$  and  $\Gamma_0$  parameters, provided that the *matching* constraints to short–distance QCD for the new Green’s functions which will appear at  $\mathcal{O}(p^6)$  can be made consistently with the LMD  $0^-, 1^-, 0^+, 1^+$  spectrum only. In fact, we have seen that at  $\mathcal{O}(p^4)$ , the *matching* constraints to short–distance QCD beyond two–point functions have actually reduced the number of three free parameters in the initial ENJL–Lagrangian *ansatz* to two. We have not yet made an exhaustive study of this important question beyond  $\mathcal{O}(p^4)$ .

One way to quantify the predictive power of the LMD approximation to  $\text{QCD}(\infty)$  which we have been considering is to fix the remaining two parameters  $M_Q$  and  $\epsilon \equiv \frac{M_Q^2}{\Lambda_\chi^2}$  (or  $\Gamma_0$ ) from a least square fit to experimentally well known quantities and compare them with the resulting predictions. The choice of low–energy constants is the one in the first column of Table 1.

**Table 1.** Low-Energy Constants, Experimental Values and Least Square Fit.

Parameter	Equation	Exp. Value	Fit Error	Predicted Value
$L_2$	(5.49)	$(1.4 \pm 0.3) \times 10^{-3}$	$\pm 0.3 \times 10^{-3}$	$1.7 \times 10^{-3}$
$L_3$	(5.49)	$(-3.5 \pm 1.1) \times 10^{-3}$	$\pm 1.1 \times 10^{-3}$	$-4.4 \times 10^{-3}$
$L_5$	(5.49)	$(1.4 \pm 0.5) \times 10^{-3}$	$\pm 0.5 \times 10^{-3}$	$1.3 \times 10^{-3}$
$L_8$	(5.49)	$(0.9 \pm 0.3) \times 10^{-3}$	$\pm 0.3 \times 10^{-3}$	$0.64 \times 10^{-3}$
$L_9$	(5.49)	$(6.78 \pm 0.15) \times 10^{-3}$	$\pm 0.15 \times 10^{-3}$	$6.8 \times 10^{-3}$
$L_{10}$	(5.49)	$(-5.13 \pm 0.19) \times 10^{-3}$	$\pm 0.19 \times 10^{-3}$	$-5.1 \times 10^{-3}$
$f_\pi$	(5.47)	$(92.4 \pm 0.3) \text{ MeV}$	$\pm 9 \text{ MeV}$	$(87 \pm 3.5) \text{ MeV}$
$\Delta m_\pi$	(5.48)	$(4.5936 \pm 0.0005) \text{ MeV}$	$\pm 0.5 \text{ MeV}$	$(4.9 \pm 0.4) \text{ MeV}$
$M_V$	(5.47)	$(768.5 \pm 0.6) \text{ MeV}$	$\pm 75 \text{ MeV}$	$(748 \pm 29) \text{ MeV}$
$M_A$	(5.47)	$(1230 \pm 40) \text{ MeV}$	$\pm 200 \text{ MeV}$	$(1058 \pm 42) \text{ MeV}$

The equations which define them in the text are given in the second column. The third column quotes their present experimental values with their errors<sup>15</sup>. The fourth column shows the errors which we have taken for the fit. The errors for the input parameters with a mass dimension are taken larger than the corresponding experimental error, to allow for possible effects due to next-to-leading  $1/N_c$ -corrections and chiral corrections. From the nine constraints in Table 1 and with the two parameters  $M_Q$  and  $\epsilon \equiv \frac{M_Q^2}{\Lambda_\chi^2}$  as free parameters we obtain a fit with a  $\chi^2 = 4.2$ . The corresponding values of the fit parameters are then

$$M_Q = (305 \pm 12) \text{ MeV}, \quad \text{and} \quad \epsilon = 0.0706 \pm 0.0031. \quad (5.50)$$

The resulting values for the  $L_i$ -constants and the other parameters are given in the last column. Typically, the errors for the predicted  $L_i$ 's are less than 2%; but of course this ignores the systematic errors of the approximation which we are adopting. Figure 8 below shows a plot of the predicted  $L'_i$ 's in eq. (5.49) versus  $\Gamma_0$ .

---

<sup>15</sup>We use the recent determination of  $L_{10}$  and the value of  $L_9$  quoted in ref. [61].

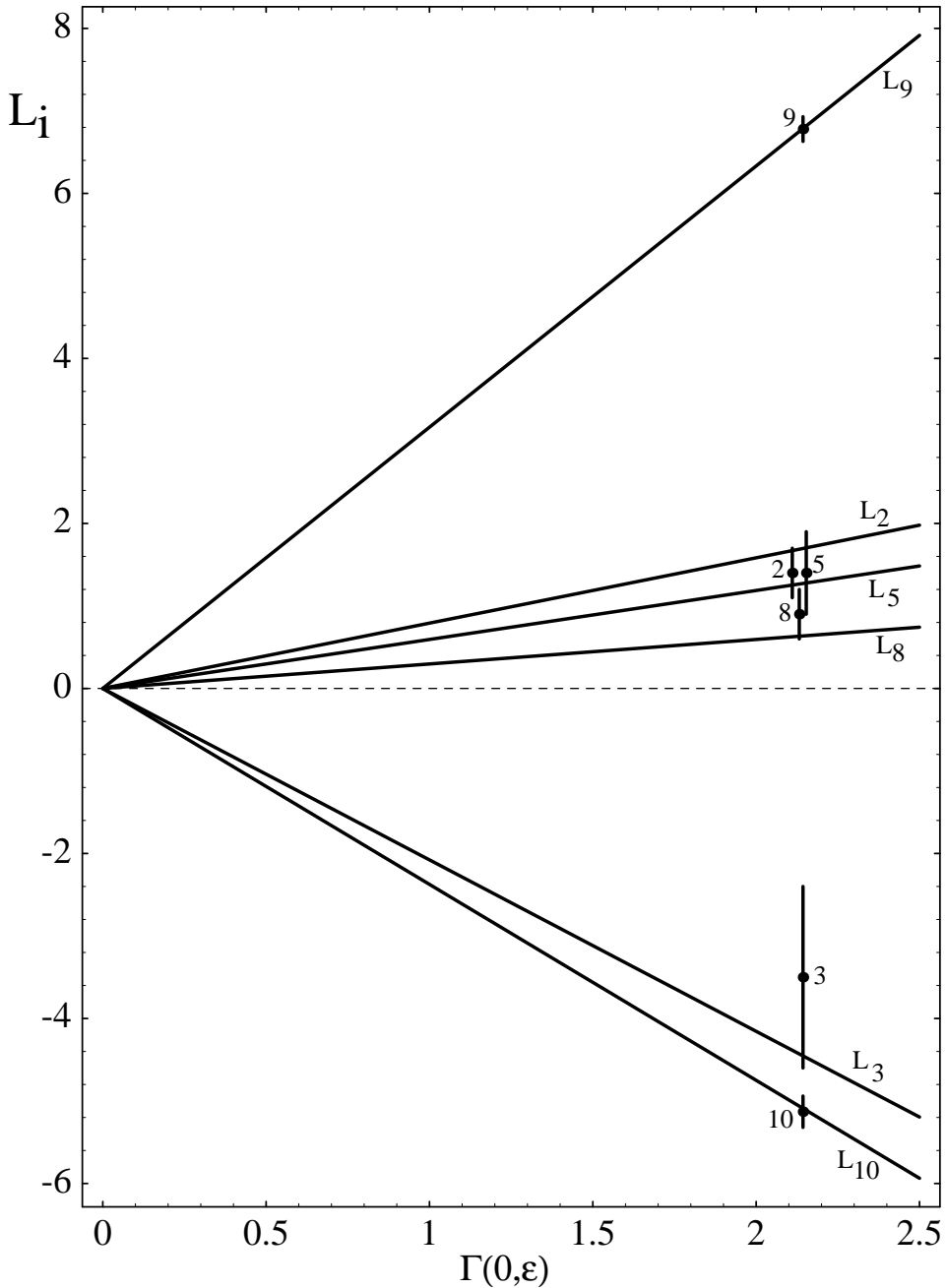


**Fig. 8** Plot of the predicted  $L_i$  constants in eq. (5.49) versus  $\Gamma_0$ . The points with error bars are the present phenomenological determination of these constants from experiment.

It is remarkable how well the phenomenological determination of these constants intercept the predicted linear dependence at the same value of  $\Gamma_0$ . This is a clear improvement, both in the quality of the fit (with one less parameter!) and in conceptual simplicity, to previous fits made with the ENJL–Lagrangian [23, 25] which were already quite good.

All the other parameters which have appeared at various stages of the discussion in the text are now fixed. For example the couplings of the initial ENJL–Lagrangian are found to

be

$$G_S = 1.28 \pm 0.01, \quad G_V = 1.65 \pm 0.04, \quad \text{and} \quad \Lambda_\chi = (1150 \pm 52) \text{ MeV}. \quad (5.51)$$

Another parameter which has been discussed in the text is the onset of the QCD continuum  $s_0$  in the vector and axial–vector spectral functions in eqs. (3.5) and (4.10). This parameter was fixed by the requirement that in the OPE of the corresponding two–point functions there is no local operator of dimension  $d = 2$  in the chiral limit. This leads to eq. (2.21) and hence, using the determination for  $f_V^2 M_V^2$  which follows from the effective Lagrangian in (5.46) fixes the value of  $s_0$  to

$$s_0(1 + \dots) = 6M_Q^2 \Gamma_0 \simeq 1.20 \text{ GeV}^2, \quad (5.52)$$

where for simplicity we have neglected gluonic perturbative corrections. Once the value of  $s_0$  is fixed, the *matching* to higher  $1/Q^2$ –powers in the OPE fixes the corresponding combinations of condensates of gauge invariant local operators. For example, *matching* the  $\frac{1}{Q^4}$  powers in the Adler function in the chiral limit, constrains the gluon condensate to satisfy the sum rule

$$\frac{1}{6} \frac{\alpha_s}{\pi} \langle G_a^{\mu\nu} G_{\mu\nu}^a \rangle = -4f_V^2 M_V^4 + \frac{N_c}{16\pi^2} \frac{4}{3} s_0^2 (1 + \dots), \quad (5.53)$$

which in terms of the two parameters  $M_Q$  and  $\Gamma_0$  and with neglect of pQCD corrections results in

$$\frac{\alpha_s}{\pi} \langle G_a^{\mu\nu} G_{\mu\nu}^a \rangle \simeq \frac{N_c}{8\pi^2} (2\sqrt{3}M_Q)^4 \Gamma_0 (\Gamma_0 - 2). \quad (5.54)$$

Numerically, this corresponds to a value

$$\alpha_s \langle G_a^{\mu\nu} G_{\mu\nu}^a \rangle \simeq 0.048 \text{ GeV}^4, \quad (5.55)$$

which is quite compatible with the phenomenological determinations (see eq. (2.14)).

Finally, the resulting shape of the Adler function, which was the starting point of our analysis after all, is the dashed curve shown in Fig. 9 below. In this curve, the gluonic corrections in the matching with the pQCD continuum have been included. The agreement with the experimental shape (the full line) is not as good as the VMD one with the experimental values of  $M_\rho$  and  $f_\rho$  plotted in Fig. 4, but it is not bad.

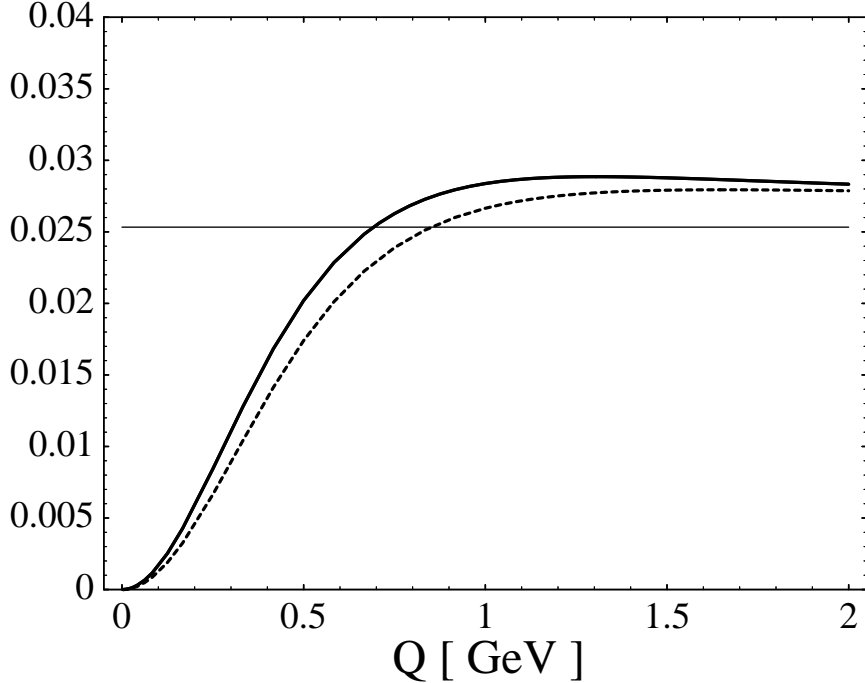


**Fig. 9** The resulting Adler function of the LMD approximation to large- $N_c$  QCD (dashed curve) compared to the experimental data (full line).

As discussed in ref. [19], in the LMD approximation to large- $N_c$  QCD, and for given values of the masses of the lowest vector and axial-vector states, all the local order parameters which appear in the OPE of the  $\Pi_{LR}(Q^2)$  correlation function are fixed by the meson masses; in particular the *matching* of the  $\frac{1}{Q^6}$  powers leads to the sum rule [19]

$$f_\pi^2 M_V^2 M_A^2 = 4\pi^2 \frac{\alpha_s}{\pi} \left( 1 + \mathcal{O}\left(\frac{\alpha_s^2}{\pi^2}\right) \right) \langle \bar{\psi} \psi \rangle^2, \quad (5.56)$$

which from eqs. (5.47) can also be written as follows

$$\frac{N_c}{4\pi^4} 9 M_Q^6 \Gamma(0, \epsilon) = \frac{\alpha_s}{\pi} \left( 1 + \mathcal{O}\left(\frac{\alpha_s^2}{\pi^2}\right) \right) \langle \bar{\psi} \psi \rangle^2. \quad (5.57)$$

Using the values for the parameters  $M_Q$  and  $\epsilon$  which result from the least square fit, i.e. the values in eq. (5.50), and the value of  $\alpha_s$  at the *matching* scale in eq. (5.52) we obtain

$$\langle \bar{\psi} \psi \rangle = [(-288 \pm 12) \text{ MeV}]^3, \quad (5.58)$$

on the high ball park of the phenomenological determinations (see eq. (2.15)) but certainly not an unreasonable value<sup>16</sup>.

One of the reasons why the ENJL-Lagrangian *ansatz* was chosen in the first place is that above the critical value  $G_S \geq 1$ , it produces a quark condensate, which in terms of  $M_Q$  and  $\epsilon$  is given by [23]

$$\langle \bar{\psi} \psi \rangle = \frac{-N_c}{16\pi^2} 4 M_Q^3 \Gamma(-1, \epsilon). \quad (5.59)$$

<sup>16</sup>In fact, the scale for the quark-condensate in eq. (5.59) is  $s_0 \simeq 1.2 \text{ GeV}^2$ , which is larger than the  $1 \text{ GeV}^2$  reference scale used in eq. (2.15). The comparison at the same  $s_0$ -scale is slightly better.

So far, however, we have not used this equation at all. *If* one is willing to identify this quark condensate to the one of  $\text{QCD}(\infty)$  at a scale  $\mu \sim \Lambda_\chi$ ; an interesting relation between the pQCD coupling constant and non-perturbative parameters appears then when inserting eq. (5.59) in the r.h.s. of eq. (5.57) and using eq. (4.11) as well:

$$\frac{\alpha_s N_c}{\pi} = \frac{9}{4} \frac{G_S^2}{G_V^2} \frac{1}{\Gamma\left(0, \frac{M_Q^2}{\Lambda_\chi^2}\right)}. \quad (5.60)$$

This relation can be viewed as a *matching* constraint between pQCD above the scale  $\Lambda_\chi$  and the non-perturbative effective realization in terms of hadronic degrees of freedom below  $\Lambda_\chi$ . [Notice that  $\Gamma\left(0, \frac{M_Q^2}{\Lambda_\chi^2}\right) = \log(\Lambda_\chi^2/M_Q^2) - \gamma_E + \dots$ .] Numerically, the central value of the r.h.s. of this equation which follows from the fit values in eqs. (5.50) and (5.51) is 0.63, while  $\frac{\alpha_s N_c}{\pi} \sim \frac{6}{11 \log(\Lambda_\chi/\Lambda_{\overline{\text{MS}}})} \simeq 0.48$ , showing that the *matching*, at least in the vector and axial-vector channels, is not unreasonable. In fact, one could use eq. (5.60) to determine  $\epsilon \equiv \frac{M_Q^2}{\Lambda_\chi^2}$ , in which case the low-energy parameters would all be constrained by just one mass scale.

## 6 Conclusions and Outlook

We have shown that there exists a useful effective Lagrangian description of a well defined approximation to QCD in the large- $N_c$  limit. This is the approximation which restricts the hadronic spectrum in the channels with  $J^P$  quantum numbers  $0^-, 1^-, 0^+$  and  $1^+$  to the lowest energy state and treats the rest of the narrow states as a  $\text{QCD}(\infty)$  perturbative continuum, the onset of the continuum being fixed by consistency constraints from the operator product expansion. The degrees of freedom in the effective Lagrangian are then a nonet of pseudoscalar Goldstone particles which are collected in a unitary matrix  $U(x)$ , and nonets of vector fields  $V(x)$ , scalar fields  $S(x)$  and axial-vector fields  $A(x)$  associated with the lowest energy states of the hadronic spectrum which are retained. We have derived the effective Lagrangian by implementing successive requirements on an ENJL-type Lagrangian (see eq. (3.1)) which we have chosen as the initial *ansatz*. The first requirement is to eliminate the effects of *non-confining*  $Q\bar{Q}$  discontinuities by introducing an infinite number of appropriate local operators with couplings which can be fixed in terms of the three parameters of the starting ENJL-Lagrangian itself, i.e.  $G_S$ ,  $G_V$  and the scale  $\Lambda_\chi$ . We have shown that the *matching* of the two-point functions of this effective Lagrangian to their QCD short-distance behaviour can be systematically implemented. In particular, the 1st and 2nd Weinberg sum rules are automatically satisfied. The resulting Adler function shown in Fig. 9, when confronted with the experimentally known curve, shows a rather good interpolation of the intermediate region between the two asymptotic regimes described by perturbative QCD (for the very short-distances) and by chiral perturbation theory (for the very long-distances).

For Green's functions beyond two-point functions, the removal of the *non-confining*  $Q\bar{Q}$  discontinuities produced by the initial ENJL *ansatz* is however not enough to guarantee in general the correct *matching* to the leading QCD short-distance behaviour and further local operators have to be included. We have discussed this explicitly in the case of the VPP and VPA three-point functions, and shown that the *matching* with the QCD short-distance leading behaviour which follows from the OPE restricts the initial three free parameters of the

ENJL–Lagrangian *ansatz* to just one mass scale  $M_Q^2$  and a dimensionless constant  $M_Q^2/\Lambda_\chi^2$ . The resulting low–energy Lagrangian in the vector and axial–vector sector, and to  $\mathcal{O}(p^4)$  in the chiral expansion, coincides with the class of phenomenological Lagrangians discussed in ref. [27] which also have two free parameters  $f_\pi^2$  and  $f_\pi^2/M_\rho^2$ . In this respect, this explains the relation to QCD of the phenomenological VMD Lagrangians discussed in ref. [27]: to  $\mathcal{O}(p^4)$ , they can be viewed as the effective low–energy Lagrangians of the LMD approximation to  $\text{QCD}(\infty)$ . On the other hand, the fact that the resulting low–energy Lagrangian coincides with the phenomenological VMD Lagrangians discussed in ref. [27] demystifies to a large extent the rôle of the ENJL–Lagrangian itself as a fundamental step in deriving the low–energy effective Lagrangian of QCD. The ENJL–Lagrangian turns out to be already a very good *ansatz* to describe in terms of quark fields degrees of freedom the LMD approximation to  $\text{QCD}(\infty)$  and this is why it is already quite successful at the phenomenological level; but, as we have seen, when the *non-confining*  $Q\bar{Q}$  discontinuities are systematically removed, the phenomenological predictions improve even more.

There is an advantage, however, in starting with the ENJL–Lagrangian as an *ansatz*, and that is that in this description of the LMD approximation to  $\text{QCD}(\infty)$ , all the couplings to all orders in  $\chi$ PT are clearly correlated to the same two free parameters. For example, as shown in eqs.(5.49), the  $L_5$  and  $L_8$  constants, as well as part of the contribution to the  $L_3$  constant which result from scalar exchanges, are now proportional to the same parameter  $\Gamma_0$ , while in a purely phenomenological description in terms of chiral effective Lagrangians which include resonances as discussed e.g. in refs. [28–31] and references therein, these low–energy constants require new phenomenological input. It is a very interesting question to ask whether or not a systematic implementation of short–distance OPE constraints on phenomenological Lagrangians leads to the same description, to all orders in the chiral expansion, as the one starting with the ENJL–Lagrangian *ansatz*. As we have said already, we have not yet undertaken this study in an exhaustive way.

Finally, we wish to insist on the phenomenological successes of the LMD approximation to  $\text{QCD}(\infty)$ , as demonstrated by the results collected in Table 1 and the plots in Figs. 8 and 9. These results show that this is indeed a very good approximation to full fledged QCD. It seems now worthwhile to apply it to the calculation of couplings of  $\mathcal{O}(p^6)$  and  $\mathcal{O}(e^2 p^2)$  as well. One can also reconsider non–leptonic weak interactions in the light of this effective Lagrangian framework, where we expect a much better *matching* between the long–distance evaluation of matrix elements of four–quark operators and the short–distance pQCD logarithmic dependence of the Wilson coefficients than e.g. in the cut–off calculations of refs. [62, 63] or the ENJL–calculations reported in ref. [64].

### Acknowledgments

We are grateful to J. Bijnens, M. Knecht and A. Pich for very helpful discussions at various stages of this work.

This work has been supported in part by TMR, EC-Contract No. ERBFMRX-CT980169 (EURODA $\phi$ NE). The work of S. Peris has also been partially supported by the research project CICYT-AEN95-0882.

### References

- [1] K. Symanzik, Commun. Math. Phys. **23** 1971) 23.
- [2] S. Weinberg, Phys. Rev. Lett. **18** (1967) 507.
- [3] S. Weinberg, Physica, **96A** 1979 327.
- [4] J. Gasser and H. Leutwyler, Ann. Phys.(N.Y.) **158** (1984) 142.
- [5] J. Gasser and H. Leutwyler, Nucl. Phys. **B250** (1985) 465.
- [6] H. Leutwyler, Ann. Phys. N.Y., **235** (1994) 65.
- [7] H.W. Fearing and S. Scherer, Phys. Rev. **D53** (1996) 315.
- [8] A. Pich, “Chiral Perturbation Theory”, Rep. Prog. Phys. **58** (1995) 563.
- [9] E. de Rafael, “Chiral Lagrangians and Kaon CP–Violation”, in *CP Violation and the Limits of the Standard Model*, Proc. TASI’94, ed. J.F. Donoghue (World Scientific, Singapore, 1995).
- [10] G. Ecker, “Chiral perturbation theory”, Prog. Part. Nucl. Phys. **35** (1995) 1.
- [11] M.A. Shifman, A.I. Vainshtein and V.I. Zakharov, Nucl. Phys. **B147** (1979) 385, 447.
- [12] H.G. Dosch and S. Narison, hep-ph/9709215.
- [13] G. ’t Hooft, Nucl. Phys. **B72** (1974) 461.
- [14] G. Rossi and G. Veneziano, Nucl. Phys. **B123** (1977) 507.
- [15] E. Witten, Nucl. Phys. **B160** (1979) 57.
- [16] E. Witten, in *Recent Developments in Gauge Theories*, eds. G. ’t Hooft et al, Plenum Press, New York and London (1980).
- [17] A. Manohar, “Large N QCD”, lectures at the Les Houches Summer School 1997, hep-ph/9802419.
- [18] S. Coleman and E. Witten, Phys. Rev. Lett. **45** (1980) 100.
- [19] M. Knecht and E. de Rafael, hep-ph/9712457, to appear in Phys. Lett. **B**
- [20] A.A. Andrianov, D. Espriu and R. Tarrach, hep-ph/9803232.
- [21] Y. Nambu and G. Jona-Lasinio, Phys. Rev. **122** (1961) 345.
- [22] A. Dahr, R. Shankar and S. Wadia, Phys. Rev. **D31** (1985) 3256.
- [23] J. Bijnens, C. Bruno and E. de Rafael, Nucl. Phys. **B390** (1993) 501.
- [24] J. Bijnens, E. de Rafael and H. Zheng, Z. Phys. **C62** (1994) 437.
- [25] J. Bijnens, Phys. Rep. **265** (1996) 369 and references therein, in particular J. Bijnens and J. Prades Z. Phys. **C64** (1994) 475, Phys. Lett. **B320** (1994) 130.
- [26] B. Moussallam, Nucl. Phys. **B504** (1997) 381.

- [27] G. Ecker, J. Gasser, H. Leutwyler, A. Pich and E. de Rafael, Phys. Lett. **B233** (1989) 425.
- [28] G. Ecker, J. Gasser, A. Pich and E. de Rafael, Nucl. Phys. **B321** (1989) 311; for a discussion of a reggeized rho meson see M. Polyakov and V. Vereshagin, Phys. Rev. **D54** (1996) 1112.
- [29] J.F. Donoghue, L. Ramirez and G. Valencia, Phys. Rev. **D39** (1989) 1947.
- [30] J.F. Donoghue, B.R. Holstein and D. Wyler, Phys. Rev. **D47** (1993) 2089.
- [31] J.F. Donoghue and A.F. Perez, Phys. Rev. **D55** (1997) 7075.
- [32] M. Polyakov and V. Vereshagin, Phys. Rev. **D54** (1996) 1112.
- [33] S. Adler, Phys. Rev. **D10** (1974) 3714.
- [34] S.G. Gorishny, A.L. Kataev and S.A. Larin, Phys. Lett. **B259** (1991) 144.
- [35] L.R. Surguladze and M.A. Samuel, Phys. Rev. Lett. **66** (1991) 560.
- [36] D. Ward, “Tests of the Standard Model: W mass and WWZ Couplings”, Talk at the HEP-Conference 97, Jerusalem, Israel 1997.
- [37] M. Davier and A. Höcker, hep-ph/9711308, to appear in Phys. Lett. .
- [38] E. Golowich and J. Kambor, Nucl. Phys. **B447** (1995) 373.
- [39] S. Peris and E. de Rafael, Nucl. Phys. **B500** (1997) 325.
- [40] A. Höcker, “Mesure des fonctions spectrales du lepton  $\tau$  et applications à la chromodynamique quantique”, *Thesis LAL 97-18*.
- [41] R.A. Bertlmann, G. Launer and E. de Rafael, Nucl. Phys. **B250** (1985) 61.
- [42] E. de Rafael, “An Introduction to Sum Rules in QCD”, lectures at the Les Houches Summer School 1997, hep-ph/9802448.
- [43] F. Le Diberder and A. Pich, Phys. Lett. **B286** (1992) 147.
- [44] A.I. Vainshtein and V.I. Zakharov, Phys. Rev. Lett. **73** (1994) 295.
- [45] A.I. Vainshtein and V.I. Zakharov, Phys. Rev. **D54** (1996) 4039.
- [46] S. Peris, Nucl. Phys. **B64** (Proc. Suppl.) (1998) 344.
- [47] N.H. Fuchs H. Sazdjian and J. Stern, Phys. Lett. **B269** (1991) 183.
- [48] J. Stern, H. Sazdjian and N.H. Fuchs, Phys. Rev. **D47** (1993) 3814.
- [49] M. Knecht, B. Moussallam, J. Stern and N.H. Fuchs, Nucl. Phys. **B457** (1995) 513.
- [50] K. Yamawaki and V.I. Zakharov, hep-ph/9406373 and hep-ph/9406399.
- [51] E. Pallante and R. Petronzio, Nucl. Phys. **B396** (1993) 205.

- [52] E. Pallante and R. Petronzio, Z. Phys. **C65** (1995) 487.
- [53] G. 't Hooft, Nucl. Phys. **B75** (1974) 461.
- [54] C.G. Callan Jr., N. Coote and D.J. Gross, Phys. Rev. **D13** (1976) 1649.
- [55] *Review of Particle Physics*, Phys. Rev. **D54** (1996).
- [56] M. Froissart, Phys. Rev. **123** (1961) 1053.
- [57] A. Martin, Phys. Rev. **129** (1963) 1432.
- [58] K. Kawarabayashi and M. Suzuki, Phys. Rev. Lett. **16** (1966) 255.
- [59] Riazuddin and Fayyazuddin, Phys. Rev. **147** (1966) 1071.
- [60] H.-N. Li and G. Sterman, Nucl. Phys. **B381** (1992) 129.
- [61] M. Davier, L. Girlanda, A. Höcker and J. Stern, hep-ph/9802447.
- [62] W.A. Bardeen, A.J. Buras and J.-M. Gérard, Nucl. Phys. **B293** (1987) 787; Phys. Lett. **B192** (1987) 138; *ibid* **B211** (1988) 343.
- [63] W.A. Bardeen *et al.*, hep-ph/9802300.
- [64] J. Bijnens and J. Prades, Nucl. Phys. **B490** (1997) 239.